

Adaptive Process Monitoring Using Covariate Information

Kai Yang and Peihua Qiu

Department of Biostatistics, University of Florida

Gainesville, FL 32610

Abstract

Statistical process control (SPC) charts provide a powerful tool for monitoring production lines in manufacturing industries. They are also used widely in other applications, such as sequential monitoring of internet traffic flows, disease incidences, health care systems, and more. In practice, quality/performance variables are often affected in a complex way by many covariates, such as material, labor, weather conditions, social/economic conditions, and so forth. Among all these covariates, some could be observed, some might be difficult to observe, and the others might even be difficult for us to notice their existence. Intuitively, an SPC chart could be improved by using helpful information in covariates. However, because of the complex relationship between the quality/performance variables and the covariates, shifts in the quality/performance variables could be due to certain covariates whose data cannot be collected. On the other hand, shifts in some observable covariates may not necessarily cause shifts in the quality/performance variables. Thus, it is challenging to properly use covariate information for process monitoring in a general setting. This paper suggests a method to handle this problem. An effective exponentially weighted moving average chart is developed, in which its weighting parameter is chosen large if the related covariates included in the collected data tend to have a shift and small otherwise. Because the covariate information is used in the weighting parameter only, the chart is designed solely for detecting shifts in the quality/performance variables, but it can react to a future shift in the quality/performance variables quickly because the helpful covariate information has been used in its observation weighting mechanism. Extensive numerical studies show that this method is effective in many different cases.

Key Words: Auxiliary variables; Covariates; Exponentially weighted moving average charts; Regression modelling; Statistical process control; Weighting function.

1 Introduction

Statistical process control (SPC) charts are widely used in industries for monitoring quality/performance variables of some sequential processes, such as the production lines, health care systems, internet traffic flows, and more. In practice, the quality/performance variables, or simply performance variables hereafter, are often associated with certain covariates. As examples, the unemployment rate of a country often depends on certain economic indices, such as inflation, GDP growth, population, and foreign direct investment; the daily number of patients with upper-respiratory conditions received by a hospital often depends on humidity, temperature, and other local weather conditions. In such applications, proper use of covariate information has the potential to improve the performance of a control chart. This paper suggests a general approach to achieve this goal.

Conventional SPC charts are originally designed for monitoring production lines in the manufacturing industry for quality control and management purposes (Qiu 2014). They are often classified into the following four groups: Shewhart charts (Shewhart 1931), cumulative sum (CUSUM) charts (Page 1954), exponentially weighted moving average (EWMA) charts (Roberts 1959), and change-point detection (CPD) charts (Hawkins et al. 2003). Early SPC research assumes that process observations are independent and identically distributed when the underlying process is in-control (IC), and that the IC process distribution has a parametric form (e.g., normal). It has been well demonstrated in the literature that a conventional SPC chart would not be reliable to use if one or more of these model assumptions are violated (Hawkins and Olwell 1998, Qiu 2014). Therefore, recent research focuses more on nonparametric or distribution-free SPC where a parametric form is not required for describing the process distribution (e.g., Chakraborti et al. 2001, Qiu 2018, Qiu and Hawkins 2001), on dynamic process monitoring where the identical distribution assumption is not imposed (e.g., Qiu and Xiang 2014, Qiu et al. 2018), and on serially correlated data monitoring where the data independence assumption is lifted (e.g., Apley and Tsung 2002, Capizzi and Masarotto 2008, Lee and Apley 2011, Qiu et al. 2020). All these control charts focus on monitoring the performance variables only, and no covariate information is taken into account in process monitoring.

In practice, performance variables of a sequential process are often affected by many different covariates, reflecting the impact of environmental and other factors on the performance of the process. In the literature, there are some existing discussions about process monitoring by

accommodating covariates, under the frameworks of risk-adjusted process monitoring (e.g., Paynabar et al. 2012, Sachlas et al. 2019, Steiner et al. 2000, Steiner and Jones 2010, Woodall et al. 2015), regression-adjusted and variable-selection-based multivariate process monitoring (e.g., Hawkins 1991, Jiang et al. 2012, Jiang et al. 2016, Peres and Fogliatto 2018, Wang and Jiang 2009, Zou and Qiu 2009, Zou et al. 2011), and cause-selecting control charts (e.g., Asadzadeh et al. 2008, Wade and Woodall 1993, Zhang 1984). These control charts are designed for some specific process monitoring problems and they are reliable to use in handling the problems that they are designed for. More specifically, the risk-adjusted process monitoring methods are mainly for the sequential monitoring of certain processes (e.g., surgeries) by adjusting the potential impact of some covariates (e.g., risk levels of patients). To use such methods, a (logistic) regression model is first built for describing the relationship between the performance variables and the covariates, and then a control chart is applied to the log-likelihood ratio scores or the residuals obtained from the estimated regression model to adjust for the covariate effect (cf., Steiner et al. 2000, Steiner and Jones 2010). The regression-adjusted and variable-selection-based multivariate process monitoring charts are for monitoring performance variables and the related covariates jointly. To use such methods, the overlapping information among all variables is first removed through regression modelling (cf., Hawkins 1991) or variable-selection (cf., Jiang et al. 2012) to improve the effectiveness of the related control charts. The cause-selecting control charts are designed for monitoring multi-stage production processes. In order to distinguish shifts at the current stage from those in the previous stage, a regression model relating the performance variables at the current stage to their values at the previous stage is first built. Then, the impact of the performance variables at the previous stage on their values at the current stage can be removed before process monitoring at the current stage (cf., Asadzadeh et al. 2008).

In many applications, our ultimate goal is to detect shifts in the performance variables promptly, and the shifts in the covariates or in the relationship between the covariates and the performance variables are either not our concern at all or our secondary concern only. For instance, in the surveillance of an infectious disease like influenza, weather conditions could be important covariates. But, we are mainly concerned about detection of disease outbreaks in this problem. If the weather information is helpful for a fast detection of disease outbreaks, then such information should be used in disease surveillance. But, shifts in weather conditions or shifts in the relationship between weather conditions and disease incidence rates are usually not our major concern. Furthermore,

shifts in weather conditions may not always result in shifts in disease incidence rates, because of their complicated relationship. In manufacturing industries, quality of products produced by a production line depends on many covariates, including workers' skill training and education level. In monitoring such production lines, we are mainly concerned about shifts in the distribution of product quality variables. Shifts in workers' skill training and education level or in their relationship with the product quality variables are often secondary. But, if the information in workers' skill training and education level is helpful for promptly detecting shifts in the product quality variables, then such information should be incorporated in process monitoring. The risk-adjusted and cause-selecting control charts described in the previous paragraph are effective for the process monitoring problems that they are designed for. However, they may not be effective for the applications mentioned above, because these charts would be sensitive to shifts in the covariates and/or in the relationship between the covariates and the performance variables. Once a signal is given by such charts, it is often difficult to judge whether the signal is due to a shift in the performance variables, a shift in the covariates, or a shift in their relationship. For the applications discussed above, the joint monitoring schemes described in the previous paragraph may not be effective either for several reasons. First, the number of covariates could be large in practice, and thus the joint monitoring problem could be complicated due to the large number of variables to monitor simultaneously. Second, after a joint monitoring scheme gives a signal, it is still unknown whether the detected shift is in the performance variables or in the covariates. Although this issue can be addressed by certain post-signal diagnostic procedures, it will complicate the entire monitoring process. More importantly, in cases when the post-signal diagnosis confirms that the detected shift is actually not in the performance variables, the interventions taken after the signal, including stopping the related process in certain applications, would waste much resource.

In this paper, we suggest an idea to make use of the helpful information in covariates when monitoring the performance variables. The proposed method is for applications in which our major task is for detecting shifts in the performance variables only, while some covariates are available and can be used as auxiliary variables. We use the EWMA charting scheme to demonstrate the suggested idea in this paper, but the same idea might also be applied to the CUSUM and CPD charting schemes. By the suggested idea, the weighting parameter of the EWMA chart for monitoring the performance variables of a process is chosen large if the covariates tend to have a shift and small otherwise. This characteristic is similar to that of an adaptive EWMA chart in the SPC

literature (Capizzi and Masarotto 2003), although the former adjusts the weighting parameter by using covariate information while the latter changes the weighting parameter value according to an estimated shift size of the performance variables. Because the suggested EWMA charting statistic is a weighted average of the current and all past observations of the performance variables, it is sensitive to shifts in the performance variables only, and would not react to shifts in the covariates and/or in the relationship between the covariates and the performance variables if such shifts do not cause any shifts in the performance variables. At the same time, because the weighting parameter of the proposed EWMA chart is chosen large when the covariates tend to have a shift, it puts most weights on the current and a few past observations and consequently it can react to a future shift in the performance variables quickly in cases when such a shift is mainly due to the covariates. Thus, the proposed chart would be more effective to detect shifts in the performance variables, compared to the corresponding charts that ignores the covariate information completely.

As a side note, it should be pointed out that the research problem discussed here is different from profile monitoring discussed in the literature (e.g., Kang and Albin 2000, Noorossana et al. 2011, Paynabar et al. 2016, Qiu et al. 2010). In profile monitoring, the major objective is to monitor the relationship between response variables and predictors over time, and the observed data at a given time point is a set of observations of the response variables and predictors (i.e., a profile). In cases with a single response variable and a single predictor, the observed data at a given time point is a set of observations of the pair (response variable, predictor) (or, a curve). In the current problem, however, the observed data at a given time point is a single vector of the performance variables and the covariates. Thus, no profiles are involved in the current problem and the existing profile monitoring methods cannot be used to solve the current problem.

The remainder of the article is organized as follows. The proposed method is described in detail in Section 2. Some simulation studies are presented in Section 3 to evaluate its numerical performance in comparison with some alternative approaches. A case study is discussed in Section 4 to demonstrate the proposed method. Several remarks conclude the article in Section 5. Some extra numerical results are provided in a supplemental file.

2 Adaptive SPC By Using Covariate Information

Assume that Y is a performance variable of a sequential process and $\mathbf{X} = (X_1, X_2, \dots, X_p)^T$ is a p -dimensional covariate vector. Their observations at time t are denoted as (\mathbf{X}_t, Y_t) . When the process is IC, assume that their observations follow the model

$$Y_t = f(\mathbf{X}_t) + \varepsilon_t, \quad \text{for } t = 1, 2, \dots, \quad (1)$$

where $f(\cdot)$ is a nonparametric regression function, and $\{\varepsilon_t, t = 1, 2, \dots\}$ are the random errors. In regression analysis, there are two different ways to handle the covariates in \mathbf{X} , i.e., they are treated as deterministic quantities or random variables. Usually, in cases when their values are pre-specified in data collection, they are treated as deterministic quantities. Otherwise, they are treated as random variables (cf., Cook and Weisberg 1999). In the current process monitoring problem, observations of \mathbf{X} are collected together with the performance variable Y . Thus, they are treated as random variables here. In model (1), it is routinely assumed that $\{\varepsilon_t\}$ are independent from $\{\mathbf{X}_t\}$. For simplicity, we further assume that the random errors are independent and identically distributed with mean zero and variance σ_ε^2 .

Let us first describe our proposed method in cases when the model (1) is linear. In such cases, $f(\mathbf{X}_t) = \beta_0 + \mathbf{X}_t^T \boldsymbol{\beta}$, for each t , where β_0 and $\boldsymbol{\beta} = (\beta_1, \beta_2, \dots, \beta_p)^T$ are regression coefficients. In such cases, the IC quantities of $\beta_0, \boldsymbol{\beta}, \sigma_\varepsilon^2$, and the mean $\boldsymbol{\mu}_\mathbf{X}$ and covariance matrix $\Sigma_\mathbf{X}$ of \mathbf{X} can be estimated from an IC dataset $\{(\tilde{\mathbf{X}}_t, \tilde{Y}_t), t = 1, 2, \dots, m\}$ of size m . More specifically, $\boldsymbol{\mu}_\mathbf{X}$ and $\Sigma_\mathbf{X}$ can be estimated by the sample mean and sample covariance matrix of the IC dataset, respectively, and $\beta_0, \boldsymbol{\beta}$, and σ_ε^2 can be estimated by the ordinary least square estimation (cf., Cook and Weisberg 1999) from the IC data. The related estimates are denoted as $\hat{\boldsymbol{\mu}}_\mathbf{X}, \hat{\Sigma}_\mathbf{X}, \hat{\beta}_0, \hat{\boldsymbol{\beta}}$, and $\hat{\sigma}_\varepsilon^2$, respectively. From (1), it can be checked that $\mu_Y = \beta_0 + \boldsymbol{\mu}_\mathbf{X}^T \boldsymbol{\beta}$ and $\sigma_Y^2 = \boldsymbol{\beta}^T \Sigma_\mathbf{X} \boldsymbol{\beta} + \sigma_\varepsilon^2$. So, they can be estimated by

$$\hat{\mu}_Y = \hat{\beta}_0 + \hat{\boldsymbol{\mu}}_\mathbf{X}^T \hat{\boldsymbol{\beta}}, \quad \hat{\sigma}_Y^2 = \hat{\boldsymbol{\beta}}^T \hat{\Sigma}_\mathbf{X} \hat{\boldsymbol{\beta}} + \hat{\sigma}_\varepsilon^2.$$

From model (1), the covariates in \mathbf{X} are associated with the performance variable Y through the regression function $f(\mathbf{X}) = \beta_0 + \mathbf{X}^T \boldsymbol{\beta}$. If the likelihood of a shift in $\mathbf{X}^T \boldsymbol{\beta}$ is large, then the likelihood of a shift in Y would also be relatively large. Based on this observation, we need to have a metric to measure the likelihood of a shift in $\mathbf{X}^T \boldsymbol{\beta}$ at the current time point t . A natural choice would be

the following EWMA charting statistic applied to the estimated and standardized values of $\mathbf{X}_t^T \boldsymbol{\beta}$:

$$E_{\mathbf{X},t} = \lambda \left[\frac{(\mathbf{X}_t - \hat{\boldsymbol{\mu}}_{\mathbf{X}})^T \hat{\boldsymbol{\beta}}}{\sqrt{\hat{\boldsymbol{\beta}}^T \hat{\boldsymbol{\Sigma}}_{\mathbf{X}} \hat{\boldsymbol{\beta}}}} \right] + (1 - \lambda) E_{\mathbf{X},t-1}, \text{ for } t \geq 1, \quad (2)$$

where $E_{\mathbf{X},0} = 0$, and $\lambda \in (0, 1]$ is a weighting parameter. From (2), the value of $E_{\mathbf{X},t}$ would be close to 0 when there is no shift in the mean of $\mathbf{X}^T \boldsymbol{\beta}$ and substantially different from 0 otherwise. Thus, the value of $E_{\mathbf{X},t}$ can be used for measuring the likelihood of a shift in $\mathbf{X}^T \boldsymbol{\beta}$. Let us assume that we are interested in detecting an upward shift in Y in a specific application. In such cases, we should focus on upward shifts in $\mathbf{X}^T \boldsymbol{\beta}$ as well due to the increasing relationship between $\mathbf{X}^T \boldsymbol{\beta}$ and Y that is described in model (1). So, the EWMA chart (2) would give a signal of an upward shift in $\mathbf{X}^T \boldsymbol{\beta}$ if

$$E_{\mathbf{X},t} > h_{\mathbf{X}}, \quad (3)$$

where $h_{\mathbf{X}} > 0$ is a control limit. For a control chart like (2)-(3), its performance is often measured by the IC average run length (ARL), denoted as ARL_0 , and the out-of-control (OC) ARL, denoted as ARL_1 . In the SPC literature, ARL_0 is defined to be the average number of observations from the beginning of process monitoring to the signal time when the process is IC, and ARL_1 is defined to be the average number of observations from the occurrence of a shift to the signal time after the process becomes OC. Usually, the value of ARL_0 is pre-specified, and the chart performs better for detecting a given shift if the value of ARL_1 is smaller. Let the ARL_0 value of the chart (2)-(3) be denoted as $ARL_{\mathbf{X},0}$. Then, the control limit $h_{\mathbf{X}}$ can be computed to achieve a pre-specified value of $ARL_{\mathbf{X},0}$ by a bootstrap procedure from the IC dataset (cf., Chatterjee and Qiu 2009).

Next, we would like to use $E_{\mathbf{X},t}$ in detecting an upward shift in Y . To this end, consider the following EWMA charting statistic:

$$E_{Y,t} = \phi(E_{\mathbf{X},t}; \lambda, h_{\mathbf{X}}) \left(\frac{Y_t - \hat{\mu}_Y}{\hat{\sigma}_Y} \right) + [1 - \phi(E_{\mathbf{X},t}; \lambda, h_{\mathbf{X}})] E_{Y,t-1}, \text{ for } t \geq 1, \quad (4)$$

where $E_{Y,0} = 0$, and $\phi(E_{\mathbf{X},t}; \lambda, h_{\mathbf{X}}) \in (0, 1]$ is a weight that depends on $E_{\mathbf{X},t}$ and $(\lambda, h_{\mathbf{X}})$. Then, the chart gives a signal of an upward shift in Y if

$$E_{Y,t} > h_Y, \quad (5)$$

where $h_Y > 0$ is a control limit chosen to achieve a pre-specified value of ARL_0 , denoted as $ARL_{Y,0}$. Once the weighting function $\phi(E_{\mathbf{X},t}; \lambda, h_{\mathbf{X}})$ and the value of $ARL_{Y,0}$ are chosen, h_Y can be determined by a bootstrap procedure from the IC dataset, similar to the determination

of the control limit $h_{\mathbf{X}}$ in (3). The chart (4)-(5) is denoted as EWMAC hereafter, indicating an EWMA chart using covariates. Note that $E_{Y,t}$ is a weighted average of the current and all previous observations of the performance variable Y by the time point t . Thus, it is sensitive to shifts in Y only, and robust to shifts in \mathbf{X} or in the relationship between \mathbf{X} and Y if such shifts do not cause shifts in Y . The chart (4)-(5) is designed for detecting upward shifts in Y . If detection of a downward or arbitrary shift in Y is our interest in a specific application, then the corresponding charts can be defined in a similar way. See Chapter 4 in Qiu (2014) for a detailed discussion.

To use the EWMAC chart (4)-(5) for detecting upward shifts in Y , we still need to choose the weighting function $\phi(E_{\mathbf{X},t}; \lambda, h_{\mathbf{X}})$. Obviously, it should be an increasing function of $E_{\mathbf{X},t}$, implying that more weight should be put on the current and nearby observations of Y when computing the charting statistic $E_{Y,t}$ if the value of $E_{\mathbf{X},t}$ is larger. In that way, the helpful information in the covariate vector \mathbf{X} can be used for a faster detection of shifts in Y . To this end, the following three functions can be considered:

$$\phi_H(x; \lambda, h_{\mathbf{X}}) = \begin{cases} 1 - (1 - \lambda)/(x/h_{\mathbf{X}}), & \text{if } x > h_{\mathbf{X}}, \\ \lambda, & \text{otherwise;} \end{cases} \quad (6)$$

$$\phi_B(x; \lambda, h_{\mathbf{X}}) = \begin{cases} \lambda + (1 - \lambda) [1 - 1/(x/h_{\mathbf{X}})^2]^2, & \text{if } x > h_{\mathbf{X}}, \\ \lambda, & \text{otherwise;} \end{cases} \quad (7)$$

and

$$\phi_L(x; \lambda, h_{\mathbf{X}}) = \begin{cases} \min \{1, \lambda + (x/h_{\mathbf{X}} - 1)\}, & \text{if } x > h_{\mathbf{X}}, \\ \lambda, & \text{otherwise.} \end{cases} \quad (8)$$

The first two functions $\phi_H(x; \lambda, h_{\mathbf{X}})$ and $\phi_B(x; \lambda, h_{\mathbf{X}})$ are the so-called Huber's function (Huber 1981) and Tukey's bisquare function (Beaton and Tukey 1974), respectively. Both of them take values in the interval $[\lambda, 1)$. The third function $\phi_L(x; \lambda, h_{\mathbf{X}})$ is linear in x when $x > h_{\mathbf{X}}$, with an upper-bound of 1. See Figure 1 for a demonstration of all three functions. From the figure, it can be seen that (i) all three functions are larger than λ when $x > h_{\mathbf{X}}$, (ii) $\phi_L(x; \lambda, h_{\mathbf{X}})$ is larger than both $\phi_H(x; \lambda, h_{\mathbf{X}})$ and $\phi_B(x; \lambda, h_{\mathbf{X}})$ when $x > h_{\mathbf{X}}$, and (iii) the two functions $\phi_H(x; \lambda, h_{\mathbf{X}})$ and $\phi_B(x; \lambda, h_{\mathbf{X}})$ are always smaller than 1, while $\phi_L(x; \lambda, h_{\mathbf{X}})$ can reach 1 when $x > (2 - \lambda)h_{\mathbf{X}}$. Among the three weighting functions, because $\phi_L(x; \lambda, h_{\mathbf{X}})$ is the largest when $x > h_{\mathbf{X}}$, the EWMAC

chart using $\phi_L(x; \lambda, h_{\mathbf{X}})$ should perform the best among the three possible EWMAC charts for detecting shifts that are strongly associated with the covariates. On the other hand, in cases when a shift to detect is not associated with the covariates at all, the charting statistic $E_{\mathbf{X},t}$ that is based solely on the covariates cannot provide any useful information for detecting the shift in Y . In such cases, the EWMAC chart using $\phi_H(x; \lambda, h_{\mathbf{X}})$ or $\phi_B(x; \lambda, h_{\mathbf{X}})$ should perform better than the one using $\phi_L(x; \lambda, h_{\mathbf{X}})$, because the weighting functions $\phi_H(x; \lambda, h_{\mathbf{X}})$ and $\phi_B(x; \lambda, h_{\mathbf{X}})$ are both closer to the constant weighting parameter λ than the weighting function $\phi_L(x; \lambda, h_{\mathbf{X}})$. Between the two weighting functions $\phi_H(x; \lambda, h_{\mathbf{X}})$ and $\phi_B(x; \lambda, h_{\mathbf{X}})$, $\phi_B(x; \lambda, h_{\mathbf{X}})$ should be a better choice than $\phi_H(x; \lambda, h_{\mathbf{X}})$ in cases when a shift in the covariates is relatively small, since $\phi_B(x; \lambda, h_{\mathbf{X}})$ would be closer to λ in such cases. These conclusions will be confirmed numerically in Section 3.

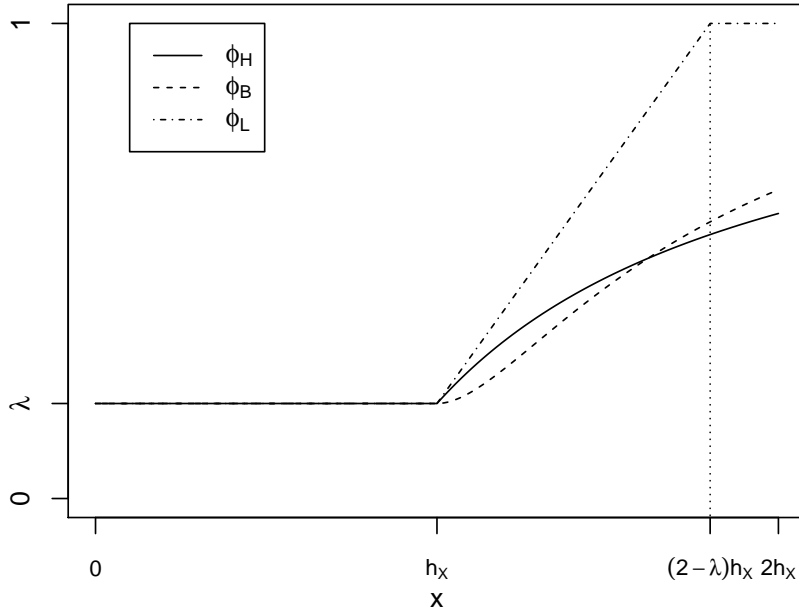


Figure 1: Demonstration of the weighting functions $\phi_H(x; \lambda, h_{\mathbf{X}})$, $\phi_B(x; \lambda, h_{\mathbf{X}})$, and $\phi_L(x; \lambda, h_{\mathbf{X}})$.

Implementation of the proposed EWMAC chart can be summarized as follows:

- i) Estimate the IC parameters $\boldsymbol{\mu}_{\mathbf{X}}, \Sigma_{\mathbf{X}}, \beta_0, \boldsymbol{\beta}$, and σ_{ε}^2 from an IC dataset.
- ii) For a given parameter λ , compute the value of $E_{\mathbf{X},t}$ by (2).
- iii) For a given value of $ARL_{\mathbf{X},0}$, determine the value of $h_{\mathbf{X}}$ in (3) by a bootstrap procedure from the IC dataset.
- iv) Choose a weighting function from the ones in (6)-(8).

- v) For a given value of $ARL_{Y,0}$, determine the value of h_Y in (5) by a bootstrap procedure from the IC dataset.
- vi) Compute the value of the charting statistic $E_{Y,t}$ by (4). The chart gives signal if (5) is true.

So, besides $ARL_{Y,0}$ which is often pre-specified, the EWMAC chart depends on the parameters λ and $ARL_{\mathbf{X},0}$ and on the weighting function $\phi_H(x; \lambda, h_{\mathbf{X}})$. Selection of these quantities will be discussed in Section 3 through numerical examples.

From the above description, implementation of the EWMAC chart (4)-(5) involves estimation of the model (1) and determination of the control limits $h_{\mathbf{X}}$ and h_Y . Next, we briefly discuss the computational complexity of these steps. When the model (1) is assumed to be linear, it can be checked that the computational complexity of its model estimation by the least squares procedure is $O(p^2m + p^3)$. In the case study discussed in Section 4, it takes about 8 and 31 seconds CPU time by the bootstrap procedure with 10,000 bootstrap replications to determine $h_{\mathbf{X}}$ and h_Y , respectively, on our Mac desktop with a 2.9 GHz Intel Core i5 processor. As a comparison, for the conventional EWMA chart with a constant weighting parameter λ , it requires $O(m)$ operations to estimate the related IC parameters, and about 8 seconds CPU time to calculate its control limit by the block bootstrap procedure with 10,000 bootstrap replications. Although the computation of the IC quantities for the EWMAC chart is a bit more demanding than that for the conventional EWMA chart, such computation is implemented for only once before online process monitoring and thus it is not a substantial burden. Once the IC quantities are computed, the online process monitoring using the EWMAC chart (4)-(5) is straightforward and its computation at each time point is trivial.

In the above description of the proposed method, the regression function $f(\mathbf{X})$ is assumed to be linear. In cases when $f(\mathbf{X})$ is nonparametric, then it needs to be estimated by some nonparametric regression methods, such as the local polynomial kernel smoothing, the smoothing spline, and the regression spline methods (Fan and Gijbels 1996, Qiu 2005, Wahba 1990), from an IC dataset. For simplicity of discussion, let us assume that there is only one covariate (i.e., $p = 1$), which is denoted as X . The observations of (X, Y) in the IC dataset are denoted as $\{(\tilde{X}_i, \tilde{Y}_i), i = 1, 2, \dots, m\}$. Then, we can consider the following local linear kernel smoothing procedure: for a given point $x \in \mathcal{X}$,

$$\min_{a, b \in \mathbb{R}^2} \sum_{i=1}^m \left\{ \tilde{Y}_i - [a + b(\tilde{X}_i - x)] \right\}^2 K \left(\frac{\tilde{X}_i - x}{h_m} \right), \quad (9)$$

where $K(u)$ is a density kernel function with the support $[-1/2, 1/2]$, $h_m > 0$ is a bandwidth, and \mathcal{X} is the interval of all possible values of X . In (9), a straight line is fitted in a neighborhood of x with width h_m by the weighted least square estimation, with the weights determined by the kernel function $K(u)$. The solution to a of the minimization problem (9) is then used for estimating $f(x)$, and it has the following expression:

$$\hat{f}(x) = \sum_{i=1}^m \tilde{Y}_i K\left(\frac{\tilde{X}_i - x}{h_m}\right) \frac{w_2 - w_1(\tilde{X}_i - x)}{w_0 w_2 - w_1^2}, \quad (10)$$

where $w_j = \sum_{i=1}^m (\tilde{X}_i - x)^j K(\frac{\tilde{X}_i - x}{h_m})$, for $j = 0, 1, 2$. In the local linear kernel smoothing procedure (9), the bandwidth h_m needs to be chosen properly in advance. Throughout this paper, the commonly used leave-one-out cross validation (LOOCV) procedure is used for this purpose. See Li and Racine (2004) for a detailed description of this procedure. Then, to use the proposed online monitoring scheme (2)-(5), the only change needed is to replace the EWMA charting statistic defined in (2) by

$$E_{X,t} = \lambda \left(\frac{\hat{f}(X_t) - \hat{\mu}_f}{\hat{\sigma}_f} \right) + (1 - \lambda) E_{X,t-1}, \text{ for } t \geq 1,$$

where $\hat{\mu}_f$ and $\hat{\sigma}_f^2$ are the sample mean and sample variance of $\{\hat{f}(\tilde{X}_i), i = 1, \dots, m\}$.

In cases when multiple covariates exist (i.e., $p > 1$), the local smoothing methods (e.g., (9)-(10)) may not work well for estimating $f(\mathbf{x})$, for $\mathbf{x} \in R^p$, because of the curse of dimensionality. In such cases, alternative approaches should be considered. One such approach is under the generalized additive model (GAM) framework (e.g., Hastie and Tibshirani 1990). Under that framework, it is assumed that $f(\mathbf{x}) = g_1(x_1) + g_2(x_2) + \dots + g_p(x_p)$, where $\mathbf{x} = (x_1, x_2, \dots, x_p)'$, and $g_1(\cdot), g_2(\cdot), \dots, g_p(\cdot)$ are univariate nonparametric functions. Compared to (1), the GAM framework might be more feasible in cases with relatively small IC data size, but the price to pay for this feasibility includes the additive structure imposed on $f(\mathbf{x})$ and the relatively intensive computation. In cases when p is large, a variable selection procedure might be needed when estimating the model (1) and constructing the EWMA charting statistic $E_{\mathbf{X},t}$. To this end, some existing variable selection methods (e.g., Fan and Li 2001, Tibshirani 1996, Zou 2006) and variable-selection-based control charts (e.g., Wang and Jiang 2010, Zou and Qiu 2010) should be helpful. In cases when the model (1) is linear and interactions among the covariates cannot be neglected, model selection and estimation become challenging, because of the large number of possible interaction terms and the hierarchical principle (i.e., lower-order terms need to be included in the model if a higher-order term is in the model) that needs to be followed in model selection. To handle such cases, Bien et

al. (2013) suggested a lasso-based approach, which should be helpful. In some applications, the performance variable Y might be multivariate, and observations of (Y, \mathbf{X}) at different time points could be correlated with a time-varying IC distribution. In such cases, the related existing research described in Section 1 should be helpful. All these issues will be addressed systematically in our future research.

3 Numerical Studies

In this section, we present some simulation results regarding the numerical performance of the proposed EWMAC chart described in Section 2. This section is organized in six parts. The first five parts are about cases when $f(x)$ in model (1) is linear, while the last part considers cases when $f(x)$ is nonparametric. More specifically, in Section 3.1, the effect of different choices of the weighting function $\phi(E_{\mathbf{X},t}; \lambda, h_{\mathbf{X}})$ (cf., (6)–(8)) on the performance of the EWMAC chart is investigated. Then, in Section 3.2, the impact of the parameters $(\lambda, ARL_{\mathbf{X},0})$ on the EWMAC chart is studied. In Sections 3.1–3.2, the IC parameters $(\beta_0, \boldsymbol{\beta})$ and the IC distributions of \mathbf{X} and Y are assumed to be known in advance. In practice, they are often unknown. Instead, we usually have an IC dataset with sample size m , and we can estimate $(\beta_0, \boldsymbol{\beta})$ from the IC dataset and search for $(h_{\mathbf{X}}, h_Y)$ by a bootstrap procedure. The impact of the IC data size m on the performance of the EWMAC chart is discussed in Section 3.3. The EWMAC chart is compared to some competing charts in Section 3.4. In Section 3.5, we investigate the performance of the EWMAC chart in cases when p is large. The performance of the EWMAC chart in cases when $f(\cdot)$ is nonparametric is studied in Section 3.6.

In Sections 3.1–3.4, it is assumed that $f(\mathbf{X}) = \beta_0 + \mathbf{X}^T \boldsymbol{\beta}$ in the IC model (1), the parameters β_0 and $\boldsymbol{\beta}$ are chosen to be 0 and $(0.5, 0.5, \dots, 0.5)^T$, and the dimension p of the covariate vector \mathbf{X} is chosen to be 1, 3, or 5. The random errors $\{\varepsilon_t\}$ are generated from the $N(0, \sigma_\varepsilon^2)$ distribution, and the observations $\{\mathbf{X}_t\}$ of the covariate vector are generated from the $N_p(\mathbf{0}, \Sigma_{\mathbf{X}})$ distribution, where $\Sigma_{\mathbf{X}} = \sigma_x^2 \mathbf{I}_{p \times p}$. In the simulation examples, unless stated otherwise, both σ_ε and σ_x are chosen to be 0.5. After the occurrence of a shift at the beginning of process monitoring, the process observations are assumed to follow the following OC model:

$$Y_t = (\beta_0 + \delta_Y) + (\mathbf{X}_t + \boldsymbol{\delta}_x)^T \boldsymbol{\beta} + \varepsilon_t, \quad (11)$$

where δ_Y is a constant, $\boldsymbol{\delta}_x = (\delta_x, \delta_x, \dots, \delta_x)^T$ is a p -dimensional vector, and the quantities $\beta_0, \boldsymbol{\beta}$, and ε_t are the same as those in the IC model (1). So, δ_x is the shift size in the mean of each covariate, and δ_Y is the shift size in the mean of Y_t that has nothing to do with the covariates. The following four types of shifts will be considered:

(I) $\delta_Y = 0.2 + 0.2\nu, \delta_x = 0$, for $\nu = 1, 2, 3, 4$;

(II) $\delta_Y = 0.2 + 0.2\nu, \delta_x = 0.025\nu$, for $\nu = 1, 2, 3, 4$;

(III) $\delta_Y = 0.025\nu, \delta_x = 0.1 + 0.05\nu$, for $\nu = 1, 2, 3, 4$;

(IV) $\delta_Y = 0, \delta_x = 0.1 + 0.05\nu$, for $\nu = 1, 2, 3, 4$.

In type (I), the covariates have no mean shift, and the mean of Y_t has four shifts with different sizes and these shifts do not depend on the covariates. In types (II) and (III), the mean shift in Y_t has two components, one is due to the covariates and the other has nothing to do with the covariates, both components have different sizes, and the one due to the covariates is smaller than the other component in type (II) while the opposite is true in type (III). In type (IV), the mean shift in Y_t is completely due to the mean shift in the covariates. Throughout this section, all ARL values are calculated from 10,000 replicated simulations unless indicated otherwise. In addition, the $ARL_{Y,0}$ value of the EWMAC chart is fixed at 200 in all examples.

3.1 Impact of different weighting functions on the EWMAC chart

In Section 2, we suggested three different weighting functions to be used in the proposed EWMAC chart. In this part, we compare the three functions in terms of the numerical performance of the EWMAC chart. To this end, let us consider cases when $p = 3$, $\lambda = 0.1, 0.3$, or 0.5 , and $ARL_{\mathbf{X},0} = 200$. In such cases, the calculated ARL_1 values of the EWMAC chart based on 10,000 replicated simulations are presented in Table 1, together with their standard errors (Note: standard error equals standard deviation of ARL divided by $\sqrt{10,000} = 100$). From the table, we can have the following conclusions. i) When the shifts are not associated with the covariates (i.e., shift type (I)), the EWMAC chart performs uniformly the best when it uses the weighting function $\phi_B(x; \lambda, h_{\mathbf{X}})$ and it performs the worst when it uses $\phi_L(x; \lambda, h_{\mathbf{X}})$ in such cases. ii) When the shifts in Y are completely due to the shifts in covariates (i.e., shift type (IV)), the chart performs

uniformly the best when it uses the weighting function $\phi_L(x; \lambda, h_{\mathbf{X}})$ and it performs the worst when it uses $\phi_B(x; \lambda, h_{\mathbf{X}})$ in such cases. iii) For shift types (II) and (III) when a mean shift in Y has two components with one due to the covariates and the other independent from the covariates, $\phi_B(x; \lambda, h_{\mathbf{X}})$ is more appropriate to use when the second component is more substantial (i.e., type (II)), while $\phi_L(x; \lambda, h_{\mathbf{X}})$ is more appropriate to use when the first component is substantially larger. iv) It seems that small λ values are good for detecting small shifts and large λ values are good for detecting large shifts for each weighting function, which is generally true for EWMA charts (cf., Qiu 2014, Chapter 5). v) It seems that the impact of different values of λ is more significant than the impact of different weighting functions. Based on this example and the analysis about the three weighting functions in Section 2, we suggest choosing the weighting function $\phi_B(x; \lambda, h_{\mathbf{X}})$ if a future shift in Y is believed to be (almost) unassociated with the covariates. On the other hand, if the future shift in Y is believed to be strongly associated with the covariates, then we suggest choosing the weighting function $\phi_L(x; \lambda, h_{\mathbf{X}})$. If we do not know the relationship between the future shift in Y and the covariates in \mathbf{X} , then any one of the three weighting functions can be used, since the performance of the proposed chart shown in Table 1 is similar across the three different weighting functions. Regarding the selection of λ , it can be pre-specified as in a conventional EWMA chart. Namely, a relatively large value is preferred if a future shift in Y is expected to be large, and a relatively small value should be used otherwise.

3.2 Impact of the parameters $(\lambda, ARL_{\mathbf{X},0})$ on the EWMAC chart

Besides the weighting function, the EWMAC chart has two parameters $(\lambda, ARL_{\mathbf{X},0})$ to choose. In this part, we study their impact on the performance of the EWMAC chart. To this end, let us consider cases when $\lambda = 0.1, 0.3$, or 0.5 , $ARL_{\mathbf{X},0} = 100, 200$, or 300 , $p = 3$, $ARL_{Y,0} = 200$, and the weighting function is chosen to be $\phi_L(x; \lambda, h_{\mathbf{X}})$. In such cases, the calculated ARL_1 values of the EWMAC chart based on 10,000 replicated simulations are presented in Table 2. From the table, we can have the following conclusions. i) The EWMAC chart performs uniformly the best when $ARL_{\mathbf{X},0} = 300$ for detecting shifts of the types (I) and (II) that either have nothing to do with the covariates or are minimally affected by the covariates, and it performs uniformly the best when $ARL_{\mathbf{X},0} = 100$ for detecting shifts of the types (III) and (IV) that are completely or mainly contributed by the covariates. ii) When the $ARL_{\mathbf{X},0}$ value and the type of shifts are given, it seems that small λ values are good for detecting small shifts and large λ values are good for detecting large

Table 1: Calculated ARL_1 values and their standard errors (in parentheses) of the EWMAC chart using one of the three different weighting functions for detecting the mean shifts in Y when $p = 3$ and $ARL_{X,0} = ARL_{Y,0} = 200$. In each row, numbers in italic denote cases with the smallest ARL_1 values when comparing different weighting functions and λ is fixed, and numbers in bold denote cases with the smallest ARL_1 values when comparing different λ values and the weighting function is fixed.

| Type ν | $\phi_B(x; \lambda, h_{\mathbf{X}})$ | | | $\phi_H(x; \lambda, h_{\mathbf{X}})$ | | | $\phi_L(x; \lambda, h_{\mathbf{X}})$ | | |
|------------|--------------------------------------|--------------------------|--------------------|--------------------------------------|-------------------|-------------------|--------------------------------------|--------------------|--------------------|
| | $\lambda = 0.1$ | $\lambda = 0.3$ | $\lambda = 0.5$ | $\lambda = 0.1$ | $\lambda = 0.3$ | $\lambda = 0.5$ | $\lambda = 0.1$ | $\lambda = 0.3$ | $\lambda = 0.5$ |
| (I) 1 | <i>14.16(0.09)</i> | <i>16.88(0.14)</i> | <i>22.02(0.20)</i> | 14.72(0.09) | 17.29(0.14) | 22.30(0.20) | 14.99(0.09) | 17.91(0.15) | 23.19(0.21) |
| 2 | <i>8.44(0.04)</i> | <i>8.67(0.06)</i> | <i>10.56(0.09)</i> | 8.71(0.04) | 8.80(0.06) | 10.68(0.09) | 8.82(0.04) | 9.02(0.06) | 10.98(0.09) |
| 3 | <i>5.92(0.02)</i> | <i>5.51(0.02)</i> | <i>6.21(0.05)</i> | 6.10(0.03) | 5.57(0.03) | 6.26(0.05) | 6.18(0.03) | 5.69(0.03) | 6.42(0.05) |
| 4 | <i>4.61(0.02)</i> | <i>3.97(0.02)</i> | <i>4.14(0.03)</i> | 4.73(0.02) | 4.01(0.02) | 4.17(0.03) | 4.79(0.02) | 4.08(0.02) | 4.27(0.03) |
| (II) 1 | <i>12.57(0.07)</i> | <i>14.53(0.11)</i> | <i>18.89(0.17)</i> | 13.07(0.08) | 14.79(0.12) | 19.12(0.17) | 13.29(0.08) | 15.31(0.12) | 19.79(0.18) |
| 2 | <i>7.27(0.04)</i> | <i>7.13(0.04)</i> | <i>8.45(0.07)</i> | 7.49(0.04) | 7.24(0.04) | 8.53(0.07) | 7.59(0.04) | 7.42(0.05) | 8.77(0.07) |
| 3 | <i>5.09(0.02)</i> | <i>4.50(0.02)</i> | <i>4.87(0.03)</i> | 5.24(0.02) | 4.56(0.02) | 4.91(0.03) | 5.31(0.02) | 4.56(0.02) | 5.01(0.03) |
| 4 | <i>3.96(0.02)</i> | <i>3.29(0.02)</i> | <i>3.29(0.02)</i> | 4.06(0.02) | 3.32(0.02) | 3.31(0.02) | 4.11(0.02) | 3.37(0.02) | 3.37(0.02) |
| (III) 1 | 20.17(0.14) | 30.31(0.27) | 41.89(0.40) | 19.42(0.13) | 29.28(0.26) | 41.00(0.39) | 19.03(0.13) | <i>28.03(0.25)</i> | <i>38.63(0.37)</i> |
| 2 | 13.29(0.08) | 18.32(0.15) | 25.67(0.24) | 12.84(0.08) | 17.68(0.15) | 25.17(0.23) | 12.63(0.07) | <i>16.92(0.14)</i> | <i>23.54(0.22)</i> |
| 3 | 9.80(0.05) | 12.18(0.09) | 16.78(0.15) | 9.52(0.05) | 11.80(0.09) | 16.45(0.15) | 9.38(0.05) | <i>11.37(0.09)</i> | <i>15.34(0.14)</i> |
| 4 | 7.74(0.04) | 8.82(0.06) | 11.61(0.10) | 7.55(0.03) | 8.55(0.06) | 11.32(0.10) | 7.46(0.03) | <i>8.20(0.06)</i> | <i>10.65(0.09)</i> |
| (IV) 1 | 21.63(0.15) | 34.23(0.31) | 47.40(0.46) | 20.61(0.14) | 32.74(0.29) | 46.15(0.44) | 20.00(0.14) | <i>30.95(0.28)</i> | <i>42.57(0.41)</i> |
| 2 | 14.68(0.09) | 22.20(0.19) | 31.85(0.30) | 14.03(0.09) | 21.09(0.18) | 30.90(0.29) | 13.64(0.08) | <i>19.51(0.17)</i> | <i>27.86(0.26)</i> |
| 3 | 10.93(0.06) | 15.20(0.12) | 21.95(0.20) | 10.48(0.06) | 14.53(0.12) | 21.31(0.19) | 10.19(0.05) | <i>13.48(0.11)</i> | <i>19.22(0.17)</i> |
| 4 | 8.72(0.04) | 11.14(0.08) | 15.97(0.14) | 8.39(0.04) | 10.64(0.08) | 15.49(0.14) | 8.15(0.04) | <i>9.87(0.07)</i> | <i>13.60(0.12)</i> |

shifts, which is consistent with the results in Table 1. iii) By comparing results for detecting shifts of the types (I)-(II) with those for detecting shifts of the types (III)-(IV), it seems that λ should be chosen smaller for detecting shifts of the types (III)-(IV) when the shifts are completely or mainly contributed by the covariates. The above conclusion ii) is generally true for EWMA charts, as mentioned in the previous part. The conclusion i) is intuitively reasonable because in cases when shifts are mainly due to the covariates, the EWMAC chart would perform better if the weighting function is larger, which can be accomplished by using a smaller $ARL_{X,0}$ value due to the facts that the control limit $h_{\mathbf{X}}$ would be smaller in such cases and consequently the weighting function would be larger (cf., Figure 1). The conclusion iii) can be explained in a similar way that a smaller λ value would result in a smaller $h_{\mathbf{X}}$ value. Consequently, the weighting function would become larger, which is favorable for detecting shifts that are mainly contributed by covariates (i.e., those of types (III) and (IV)). This example shows that both $ARL_{X,0}$ and λ should be chosen small if a future shift in Y is mainly due to the covariates, and relatively large otherwise. We also considered

cases when $p = 1$ or 5 and other setups are the same as those in Table 2. The corresponding results are presented in the supplemental file, and similar conclusions to those in Table 2 can be made.

Table 2: Calculated ARL_1 values and their standard errors (in parentheses) of the EWMAC chart when the weighting function is chosen to be $\phi_L(x; \lambda, h_{\mathbf{X}})$, $ARL_{Y,0} = 200$, and $p = 3$. In each row, numbers in italic denote cases with the smallest ARL_1 values when comparing different $ARL_{0,\mathbf{X}}$ values with λ fixed, and numbers in bold denote cases with the smallest ARL_1 values when comparing different λ values with $ARL_{0,\mathbf{X}}$ fixed.

| Type ν | $ARL_{\mathbf{X},0} = 100$ | | | $ARL_{\mathbf{X},0} = 200$ | | | $ARL_{\mathbf{X},0} = 300$ | | |
|------------|----------------------------|--------------------|--------------------|----------------------------|-------------------|-------------------|----------------------------|--------------------|--------------------|
| | $\lambda = 0.1$ | $\lambda = 0.3$ | $\lambda = 0.5$ | $\lambda = 0.1$ | $\lambda = 0.3$ | $\lambda = 0.5$ | $\lambda = 0.1$ | $\lambda = 0.3$ | $\lambda = 0.5$ |
| (I) 1 | 21.19(0.14) | 20.24(0.17) | 25.86(0.24) | 14.99(0.09) | 17.91(0.15) | 23.19(0.21) | 14.07(0.09) | <i>17.21(0.14)</i> | <i>22.64(0.21)</i> |
| 2 | 11.40(0.06) | 9.87(0.06) | 12.05(0.10) | 8.82(0.04) | 9.02(0.06) | 10.98(0.09) | 8.40(0.04) | <i>8.78(0.06)</i> | <i>10.80(0.09)</i> |
| 3 | 7.73(0.03) | 6.10(0.03) | 6.87(0.05) | 6.18(0.03) | 5.69(0.03) | 6.42(0.05) | <i>5.90(0.03)</i> | 5.55(0.03) | <i>6.32(0.05)</i> |
| 4 | 5.86(0.02) | 4.32(0.02) | 4.51(0.03) | 4.79(0.02) | 4.08(0.02) | 4.27(0.03) | <i>4.60(0.02)</i> | 4.00(0.02) | <i>4.20(0.03)</i> |
| (II) 1 | 18.12(0.11) | 17.18(0.11) | 21.70(0.20) | 13.29(0.08) | 15.31(0.12) | 19.79(0.18) | 12.50(0.07) | <i>14.75(0.12)</i> | <i>19.41(0.18)</i> |
| 2 | 9.63(0.05) | 8.08(0.05) | 9.48(0.08) | 7.59(0.04) | 7.42(0.04) | 8.76(0.07) | <i>7.24(0.03)</i> | 7.21(0.05) | <i>8.63(0.07)</i> |
| 3 | 6.52(0.02) | 4.97(0.02) | 5.31(0.03) | 5.31(0.02) | 4.65(0.02) | 5.01(0.03) | <i>5.07(0.02)</i> | 4.54(0.02) | <i>4.95(0.03)</i> |
| 4 | 4.98(0.02) | 3.55(0.02) | 3.53(0.02) | 4.11(0.02) | 3.37(0.02) | 3.36(0.02) | <i>3.95(0.02)</i> | <i>3.33(0.02)</i> | 3.31(0.02) |
| (III) 1 | 17.34(0.12) | <i>25.54(0.23)</i> | <i>35.69(0.33)</i> | 19.03(0.13) | 28.03(0.25) | 38.63(0.37) | 20.05(0.14) | 29.08(0.26) | 40.11(0.38) |
| 2 | 11.72(0.07) | <i>15.60(0.13)</i> | <i>22.16(0.20)</i> | 12.63(0.07) | 16.92(0.14) | 23.54(0.21) | 13.24(0.08) | 17.50(0.15) | 24.38(0.23) |
| 3 | 8.76(0.05) | <i>10.55(0.08)</i> | <i>14.26(0.13)</i> | 9.38(0.05) | 11.37(0.08) | 15.34(0.14) | 9.78(0.05) | 11.75(0.09) | 15.99(0.14) |
| 4 | 7.01(0.03) | <i>7.68(0.05)</i> | <i>9.98(0.08)</i> | 7.46(0.03) | 8.20(0.06) | 10.65(0.09) | 7.73(0.04) | 8.48(0.06) | 10.99(0.09) |
| (IV) 1 | 17.88(0.12) | <i>27.32(0.24)</i> | <i>39.17(0.37)</i> | 20.00(0.14) | 30.95(0.28) | 42.57(0.41) | 21.47(0.15) | 32.30(0.29) | 44.79(0.43) |
| 2 | 12.30(0.07) | <i>17.58(0.15)</i> | <i>25.47(0.23)</i> | 13.64(0.08) | 19.52(0.17) | 27.86(0.25) | 14.54(0.10) | 20.72(0.19) | 29.40(0.29) |
| 3 | 9.30(0.05) | <i>12.10(0.09)</i> | <i>17.40(0.16)</i> | 10.19(0.05) | 13.48(0.11) | 19.22(0.17) | 10.83(0.06) | 14.20(0.12) | 20.20(0.19) |
| 4 | 7.47(0.04) | <i>8.92(0.06)</i> | <i>12.45(0.11)</i> | 8.15(0.04) | 9.87(0.07) | 13.60(0.12) | 8.64(0.04) | 10.42(0.08) | 14.39(0.13) |

3.3 Impact of the IC data size m on the EWMAC chart

In the proposed EWMAC chart, the IC parameters, including $(\beta_0, \boldsymbol{\beta})$ in model (1) and the control limit h_Y in (5), need to be estimated from an IC dataset of size m . So, its performance would depend on m . Generally speaking, the larger the IC data size, the better the performance of the EWMAC chart. But, what is the necessary IC data size to have a reliable performance of the EWMAC chart? To answer this question, we perform a numerical study, in which m changes from 100 to 800 with a constant step of 100, $p = 1, 3$ or 5 , $\beta_0 = 0$, $\boldsymbol{\beta} = (0.5, 0.5, 0.5)^T$, $\sigma_\varepsilon = \sigma_x = 0.5$, $ARL_{\mathbf{X},0} = ARL_{Y,0} = 200$, $\lambda = 0.1, 0.3$ or 0.5 , and other setups are the same as those in the example of Table 2. To run a simulation, we first generate an IC dataset of size m from model (1). Then, the regression coefficients $(\beta_0, \boldsymbol{\beta})$ are estimated from the IC data, and the parameters $(h_{\mathbf{X}}, h_Y)$ are computed from the IC dataset by bootstrap with a bootstrap sample size of 10,000. Then,

10,000 observations are generated from the OC model, the EWMAC chart is used for monitoring these observations, and the number of observation times from the beginning of monitoring to the first signal from the chart is recorded as a run length (RL) value. This sequential monitoring process is repeated for 10,000 times, and the average of the 10,000 RL values can be regarded as the actual ARL value. Because this ARL value depends on the initial IC dataset, we repeat the entire simulation mentioned above, including generation of the initial IC dataset, estimation of $(\beta_0, \boldsymbol{\beta})$, determination of $(h_{\mathbf{X}}, h_Y)$, and computation of ARL , for 1,000 times to reduce the randomness in the results. Then, the average of the 1,000 ARL values is used as the final estimate of the actual ARL value. We first studied the IC performance of the EWMAC chart, by setting all related shifts to be 0. The computed actual $ARL_{Y,0}$ values are shown in Figure 2, where the shaded area in each plot denotes $ARL_{Y,0}$ values that are within 5% of the nominal level of 200. From the plots in the figure, it can be seen that i) the difference between the actual and nominal $ARL_{Y,0}$ values gets smaller when m is larger, ii) their difference depends on p and λ , and the difference would be smaller if p is smaller or λ is larger, and iii) the difference would be within 5% of the nominal level if $m \geq 400$ in all cases considered. In this example, we also investigated the sampling variability by calculating the standard deviation of the 1,000 IC ARL values, denoted as $SDARL_{Y,0}$. The smaller the $SDARL_{Y,0}$ value, the more stable the IC performance of the control chart. The calculated $SDARL_{Y,0}$ values are presented in Figure S.1 of the supplementary file. From the plots of the figure, it can be seen that i) the chart with larger weighting parameter λ has more sampling variability, which is consistent with the conclusion in Saleh et al. (2015), ii) $SDARL_{Y,0}$ values are generally larger when p increases, and iii) $SDARL_{Y,0}$ becomes smaller when m is larger and $SDARL_{Y,0}$ would be within 15% of the nominal $ARL_{Y,0}$ value of 200 in all cases considered when $m \geq 400$. From the results in Figures 2 and S.1, it seems that the control chart would have a stable IC performance when $m \geq 400$ in this example. In addition, we studied the impact of m on the OC performance of the EWMAC chart, by comparing the actual ARL_1 values, computed in a similar way to that described above when computing the actual $ARL_{Y,0}$ values, and the nominal ARL_1 values, computed in cases when the true model (1) was assumed known. It was found that the actual ARL_1 values would be within 5% of the corresponding nominal ARL_1 values when $m \geq 100$ for detecting the four types of shifts considered in the previous examples.

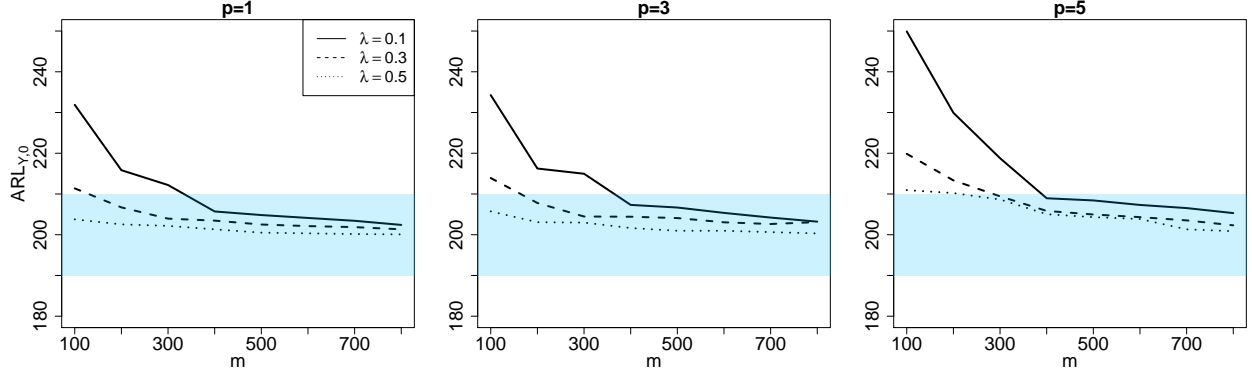


Figure 2: Actual $ARL_{Y,0}$ values of the EWMAC chart when the IC data size m changes from 100 to 800, the nominal $ARL_{Y,0}$ value is 200, and $p = 1, 3$ or 5 . Shaded area in each plot denotes $ARL_{Y,0}$ values that are within 5% of the nominal level of 200.

3.4 Comparison with some alternative control charts

In this part, we compare the proposed EWMAC chart with some alternative control charts described below. First, we consider the conventional upward EWMA chart that monitors the performance variable Y only and ignores the covariates in \mathbf{X} completely. This chart can be accomplished by the chart (4)-(5) after the weighting function $\phi(E_{\mathbf{X},t}; \lambda, h_{\mathbf{X}})$ is replaced by the constant λ , and it is denoted as EWMA here. Second, the adaptive EWMA chart suggested by Capizzi and Masarotto (2003), denoted as AEWMA, is considered here. The major idea of AEWMA is to determine its weighting parameter value according to an estimated shift size at the current time point. In the chart, a score function is needed to turn the estimated shift size to a legitimate weight. The recommended score function in Capizzi and Masarotto (2003) is used in this part. Third, it is natural to monitor both the performance variable Y and all covariates in \mathbf{X} simultaneously. To this end, we consider using the general multivariate EWMA chart suggested by Lowry et al. (1992), which is briefly described below. Let $\mathbf{Y}_t^* = (Y_t, \mathbf{X}_t^T)^T$ and $\boldsymbol{\mu}_{\mathbf{Y}^*}$ and $\Sigma_{\mathbf{Y}^*}$ be its IC mean and IC covariance matrix. Both $\boldsymbol{\mu}_{\mathbf{Y}^*}$ and $\Sigma_{\mathbf{Y}^*}$ can be estimated from the IC data. The estimates are denoted as $\hat{\boldsymbol{\mu}}_{\mathbf{Y}^*} = (\hat{\mu}_Y, \hat{\boldsymbol{\mu}}_{\mathbf{X}}^T)^T$ and $\hat{\Sigma}_{\mathbf{Y}^*}$, respectively. Then, the multivariate EWMA charting statistic is defined as

$$T_t = \mathbf{E}_t^T \hat{\Sigma}_{\mathbf{Y}^*}^{-1} \mathbf{E}_t, \text{ where } \mathbf{E}_t = \lambda(\mathbf{Y}_t^* - \hat{\boldsymbol{\mu}}_{\mathbf{Y}^*}) + (1 - \lambda)\mathbf{E}_{t-1},$$

where λ is a weighting constant. The chart gives a signal when T_t is larger than a control limit. The above multivariate EWMA chart is designed for detecting arbitrary shifts. Because the proposed

EWMAC chart is designed for detecting upward shifts in Y only, to make them comparable, the above multivariate EWMA chart should be modified for detecting upward shifts in Y as well. To this end, we consider the following modification: whenever the first element of \mathbf{E}_t is negative, the entire vector of \mathbf{E}_t is reset to $\mathbf{0}$. In that way, the downward shifts in Y could hardly be detected by the modified chart because they would most probably make the first element of \mathbf{E}_t negative. This modified multivariate EWMA chart is denoted as MEWMA. Fourth, we consider a risk-adjusted control chart that shares a similar idea to that of the EWMA chart in Steiner and Jones (2010) which uses the observed minus expected deaths scores when constructing its charting statistic. To this end, a regression model is first built from the IC dataset, with Y as response and \mathbf{X} as predictors. Then, for online process monitoring, the conventional EWMA chart for detecting upward shifts is applied to the residuals $\{\hat{\varepsilon}_t\}$ of Phase II observations calculated using the estimated regression model. The resulting control chart is denoted as RA. Fifth, we consider the regression-adjusted multivariate control chart suggested by Hawkins (1991) for monitoring Y and \mathbf{X} jointly. To use this chart, the overlapping information in individual variables should be deleted first, as discussed in Section 1. This chart is denoted as ZNO. Finally, we consider a cause-selecting control chart, denoted as CSC. The CSC charting scheme consists of two control charts, referred to as the X-chart and Z-chart (cf., Asadzadeh 2008). The X-chart is used to monitor the covariates in \mathbf{X} , and it is chosen to be the conventional EWMA chart if $p = 1$ and the multivariate EWMA chart proposed by Lowry et al. (1992) otherwise. The Z-chart is used to monitor the residuals $\{\hat{\varepsilon}_t\}$ mentioned above, and it is chosen to be the conventional EWMA chart. The entire CSC charting scheme gives a signal when at least one of the two charts gives a signal. It should be pointed out that all these alternative control charts are designed for purposes that are different from the one of the proposed method. The main reason to consider them here is to show that they are ineffective to solve the current research problem and thus the proposed method is needed.

To compare the seven charts EWMAC, EWMA, AEWMA, MEWMA, RA, ZNO and CSC, we consider cases when $p = 3$, $\beta = 0.5$, $\sigma_\varepsilon = \sigma_x = 0.5$, $m = 400$, and $ARL_0 = 200$ in all charts, and the other setups are the same as those in the example of Table 2. For the RA and CSC charts, the least-square method is used when estimating all the regression coefficients in the linear regression model $Y_t = \beta_0 + \mathbf{X}_t^T \boldsymbol{\beta} + \varepsilon_t$. The IC parameters in all charts are estimated from the IC data in advance and their control limits are determined by the bootstrap procedure with the bootstrap sample size of 10,000 from the IC data. To make the comparison fair, we focus on the optimal

performance of all charts. Namely, to detect a given shift, the parameters (e.g., the weighting parameter λ or the allowance constant k) of the charts are chosen such that their ARL_1 values reach the minimum. Otherwise, their performance may not be comparable, if λ and k are chosen to be the same in all charts. See a related discussion about this issue in Qiu (2018). The calculated optimal ARL_1 values of the seven charts are shown in Figure 3. It can be seen from the figure that i) the proposed EWMAC chart is better than the other six charts for detecting shifts of types (III) and (IV) when the shifts in Y are mainly or completely due to shifts in the covariates, ii) the EWMAC chart performs almost the same as the charts EWMA, AEWMA, CSC, MEWMA and ZNO when detecting shifts of types (I) and (II), and slightly worse than RA in such cases, and iii) the RA chart performs the best when detecting shifts of types (I) and (II), but poorly for detecting shifts of types (III) and (IV). The last conclusion is expected because the shifts of types (I) and (II) are not or minimally related to covariates and the variability of the risk-adjusted residuals would be smaller than that of the original observations of Y . Thus, the related chart based on the residuals would be more effective than the chart based on the original observations of Y . However, for detecting shifts of types (III) and (IV) that are mainly or completely due to the covariates, RA has little power because the risk-adjusted residuals contain little information about the shifts after the covariate effect is deducted from the original observations of Y . This example confirms that the proposed chart EWMAC is effective in detecting shifts in Y , after the helpful information in \mathbf{X} has been taken into account. Even in cases when a potential shift in Y has nothing to do with the covariates in \mathbf{X} (cf., the top-left panel in Figure 3), EWMAC would not lose much power in detecting such a shift because the weighting function $\phi(E_{\mathbf{X},t}; \lambda, h_{\mathbf{X}})$ used in (4) would be the same as λ due to the fact that $E_{\mathbf{X},t}$ is likely smaller than $h_{\mathbf{X}}$ in such cases. As a comparison, the risk-adjusted chart RA could be unreliable to use in cases when the shift in Y is mainly due to the covariates in \mathbf{X} .

3.5 Cases when p is large

In the numerical examples presented in the previous parts, p is chosen to be 1, 3 or 5, which is quite small. In this part, we study the performance of the EWMAC chart in some cases when p is large. To this end, let us consider cases when $p = 50$, the first 10 elements of β are all 0.5, and the remaining elements are 0. The other setups are the same as those in Table 2. In such cases, the regression model (1) can be estimated by a Lasso-based model fitting procedure, which can be accomplished

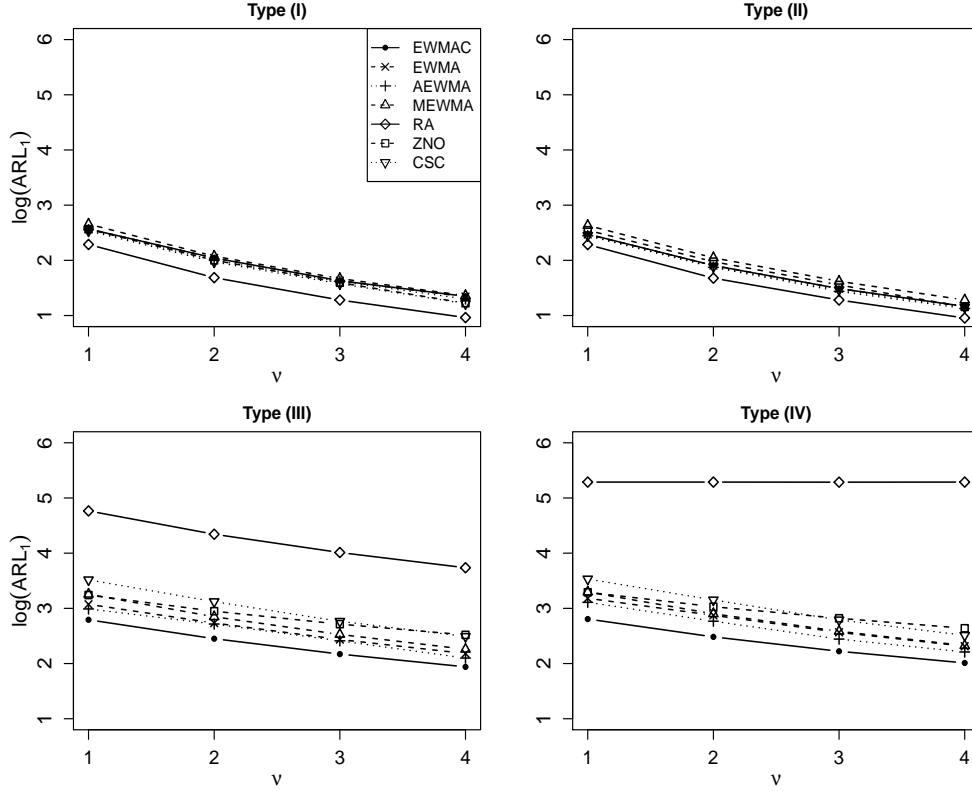


Figure 3: Calculated optimal ARL_1 values of the seven charts EWMAC, EWMA, AEWMA, MEWMA, RA, ZNO and CSC for detecting shifts of types (I)–(IV) when $p = 3$. Note that the y -axis in each plot is in log scale.

by using the function `glmnet()` in the R package `glmnet` where the tuning parameter is chosen by the 10-fold cross-validation. First, let us study the impact of $(\lambda, ARL_{X,0})$ on the performance of the EWMAC chart in cases when $\sigma_\varepsilon = \sigma_x = 0.5$, $\lambda = 0.1, 0.3$ or 0.5 , $ARL_{0,X} = 100, 200$ or 300 , and $ARL_{0,Y} = 200$. The calculated ARL_1 values based on 10,000 replicated simulations are presented in the supplementary file. It can be seen that similar conclusions to those from Table 2 can be made here. Second, we study the impact of the IC sample size m on the performance of the EWMAC chart by changing m from 100 to 800. The calculated actual $ARL_{Y,0}$ values of EWMAC are shown in Figure 4. From the figure, we can see that the actual $ARL_{Y,0}$ value would be within 5% of the nominal $ARL_{Y,0}$ level of 200 when $m \geq 600$. We also computed the $SDARL_{Y,0}$ values of the EWMAC chart, which are shown in Figure S.2 of the supplementary material. From the figure, it can be seen that the $SDARL_{Y,0}$ values are within 15% of the nominal $ARL_{Y,0}$ of 200 when $m \geq 600$. In addition, we find that the actual ARL_1 values could be within 5% of the corresponding

nominal ARL_1 values (i.e., the ARL_1 values when the model (1) is assumed known) when $m \geq 300$ for detecting shifts of types (I)-(IV) considered earlier. By comparing these results with those in Section 3.3, it can be seen that more IC data are required to have a reliable performance of the EWMAC chart when p is larger.

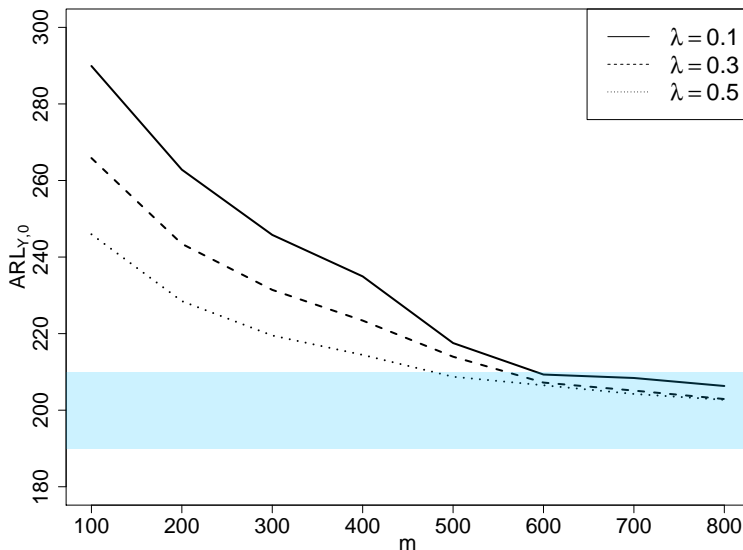


Figure 4: Actual $ARL_{Y,0}$ values of the EWMAC chart when the IC data size m changes from 100 to 800, the nominal $ARL_{Y,0}$ value is 200, $p = 50$, and $\lambda = 0.1, 0.3$ and 0.5 . Shaded area denotes the $ARL_{Y,0}$ values that are within 5% of the nominal level of 200.

Finally, the proposed EWMAC chart is compared with the six competing charts EWMA, AEWMA, MEWMA, RA, ZNO and CSC in this example when m is fixed at 600 and all other setups keep the same as those in Section 3.4. To make the comparison as fair as possible, the model (1) is estimated by the R-function `glmnet()` for the three charts EWMAC, RA and CSC that depend on that model. In all the seven control charts, the ARL_0 value is fixed at 200, and their control limits are determined by the bootstrap procedure with the bootstrap sample size of 10,000. Their calculated optimal ARL_1 values for detecting shifts of the types (I)-(IV) are presented in Figure 5. From the plots of the figure, it can be seen that similar conclusions to those from Figure 3 can be made here, and the proposed EWMAC chart still performs well in this example when p is relatively large.

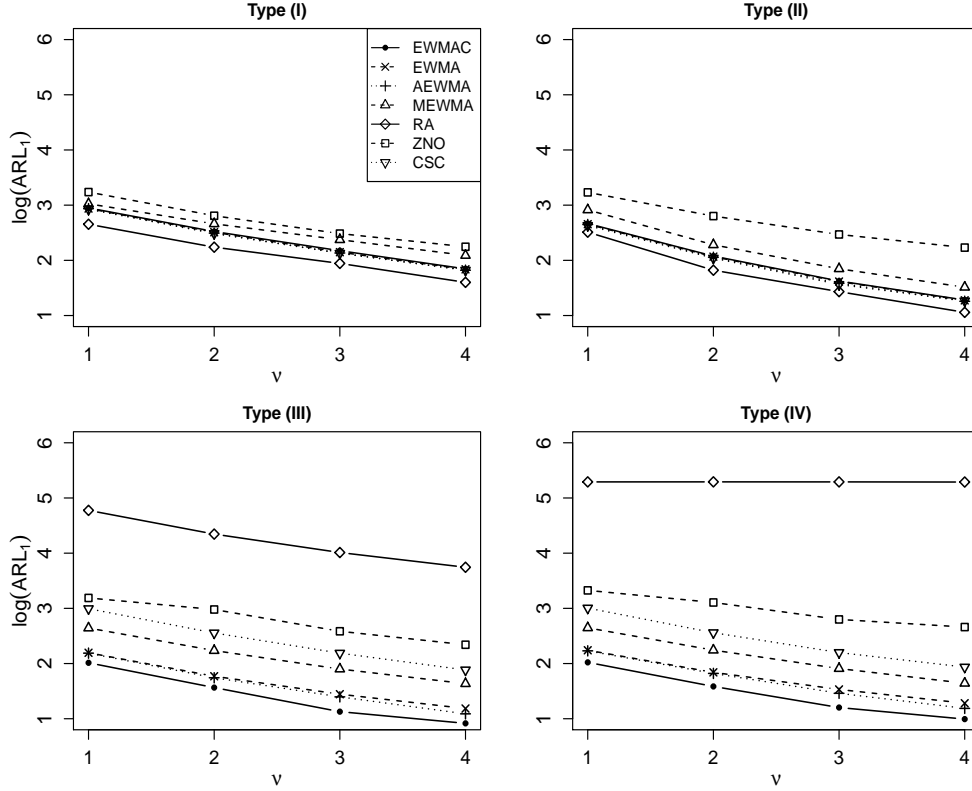


Figure 5: Calculated optimal ARL_1 values of the seven charts EWMAC, EWMA, AEWMA, MEWMA, RA, ZNO and CSC for detecting shifts of types (I)–(IV) when $p = 50$. Note that the y -axis in each plot is in log scale.

3.6 Cases when $f(\mathbf{X})$ is nonparametric

In the previous parts, $f(\mathbf{X})$ is assumed to be linear. In this part, we consider some cases when $f(\mathbf{X})$ is nonparametric and study the performance of the proposed EWMAC chart in such cases. To this end, let us consider cases when $p = 1$ and $f(x) = 0.5 \exp(x)$. In such cases, $f(x)$ is estimated by the local linear kernel smoothing procedure (9)–(10) and the corresponding EWMAC chart is described in the paragraph with Equation (10) in Section 2. First, we investigate the impact of $(\lambda, ARL_{\mathbf{X},0})$ on the performance of the proposed EWMAC chart in cases when $\sigma_\varepsilon = \sigma_x = 0.5$, $\lambda = 0.1, 0.3$ or 0.5 , $ARL_{0,X} = 100, 200$ or 300 , $ARL_{0,Y} = 200$, and the other setups are the same as those in the example of Table 2. The calculated ARL_1 values based on 10,000 replications are presented in the supplemental file. Similar conclusions to those in Section 3.2 (cf., Table 2) can be made from this table. More specifically, it can be seen from the table that i) the EWMAC chart performs the best when $ARL_{0,X} = 300$ for detecting shifts of the types (I) and (II), and it performs the best

when $ARL_{0,\mathbf{X}} = 100$ for detecting shifts of the types (III) and (IV), ii) small λ values are good for detecting small shifts and large λ values are good for detecting large shifts, and iii) for detecting shifts that are mainly or completely due to shifts in covariates (i.e., shifts of the types (III) and (IV)), λ should be chosen relatively small to have a good shift detection performance.

Next, we study the effect of the IC sample size m on the performance of the EWMAC chart. In the above example, let $m = 100, 200, \dots, 800$, and all other setups are kept unchanged. Then, the calculated actual $ARL_{Y,0}$ values of EWMAC are presented in Figure 6, where the shaded area denotes the $ARL_{Y,0}$ values that are within 5% of the nominal $ARL_{Y,0}$ level of 200. From Figure 6, it can be seen that it is enough to have $m \geq 400$ to ensure that the actual $ARL_{Y,0}$ values are within 5% of the nominal level of 200 in all cases considered. In addition, we calculated the $SDARL_{Y,0}$ values of EWMAC and the results were presented in Figure S.3 of the supplementary file. From the figure, the $SDARL_{Y,0}$ values are all within 15% of the nominal $ARL_{Y,0}$ value of 200 when $m \geq 400$. Also, we find that the actual ARL_1 values are within 5% of the corresponding nominal ARL_1 values when $m \geq 100$ for detecting all four types of shifts (I)-(IV) considered in the example of Table 1. This part of the results is omitted here to save some space.

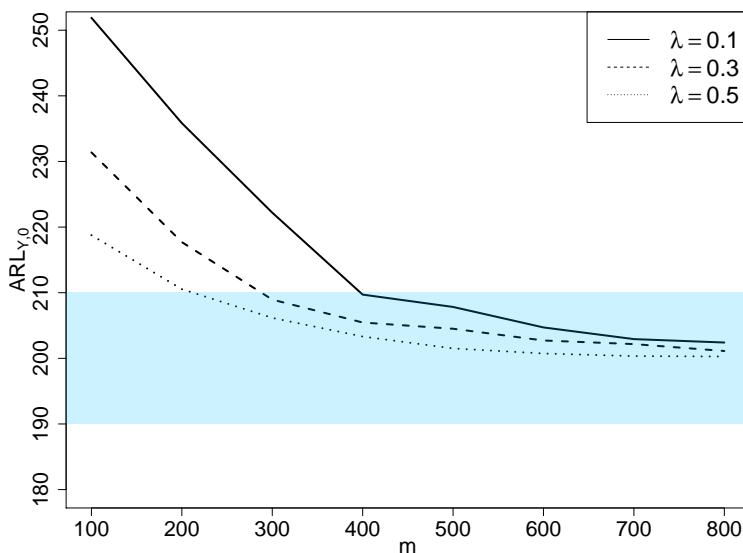


Figure 6: Actual $ARL_{Y,0}$ values of the EWMAC chart when the IC data size m changes from 100 to 800, the nominal $ARL_{Y,0}$ value is 200, $p = 1$, $f(x) = 0.5 \exp(x)$ and $\lambda = 0.1, 0.3$ and 0.5 . Shaded area denotes the $ARL_{Y,0}$ values that are within 5% of the nominal level of 200.

Finally, we compare the performance of the seven chart EWMAC, EWMA, AEWMA, MEWMA,

RA, ZNO and CSC in this example when m is fixed at 400 and the charts are set up in the same way as that in Section 3.4. To make the comparison as fair as possible, the nonparametric regression function $f(x)$ is estimated by the local linear kernel smoothing procedure (9)-(10) for the charts EWMAC, RA and CSC. In all charts, the ARL_0 value is fixed at 200, and their control limits are determined by the bootstrap procedure with the bootstrap sample size of 10,000. The calculated optimal ARL_1 values of the seven charts are shown in Figure 7, and similar conclusions to those from Figure 3 in Section 3.4 can be made here. Thus, results in this part confirm that the proposed chart EWMAC performs well in cases when $f(x)$ is nonparametric.

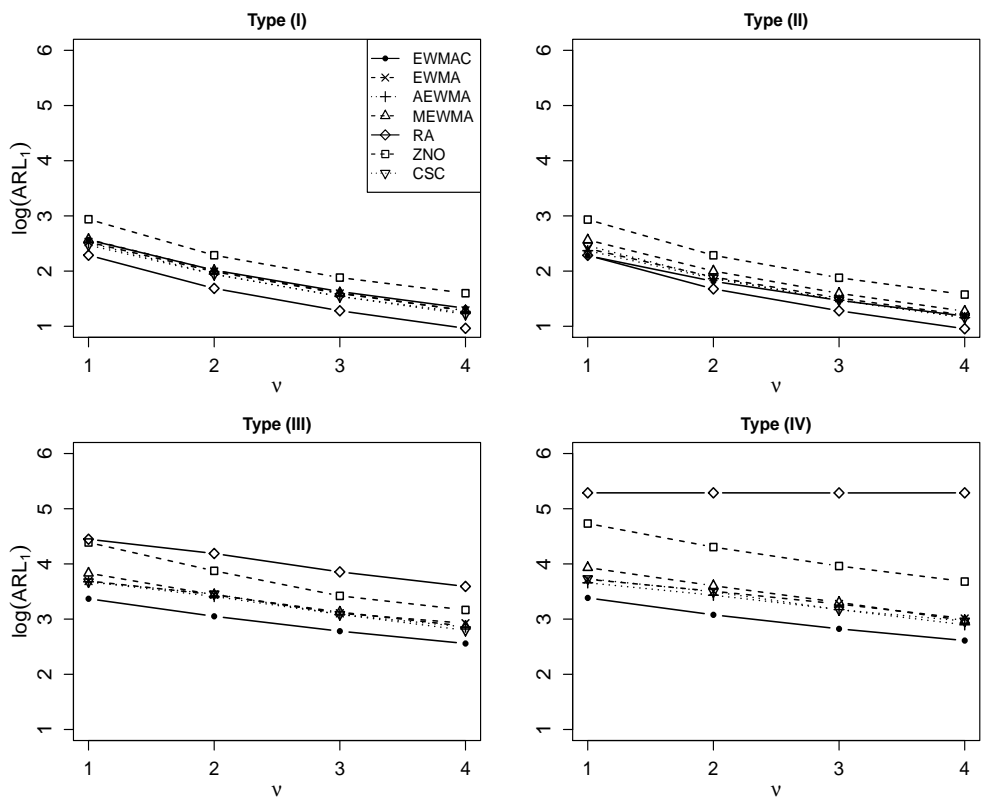


Figure 7: Calculated optimal ARL_1 values of the seven charts EWMAC, EWMA, AEWMA, MEWMA, RA, ZNO and CSC for detecting shifts of types (I)–(IV) when $p = 1$ and $f(x) = 0.5 \exp(x)$. Note that the y -axis in each plot is in log scale.

4 Case Study

In this section, we apply the related control charts to a case study about the weekly initial jobless claims (Y) in Arizona. By definition, the initial jobless claims in Arizona in the current week are referred to those individuals who filed for state unemployment insurance for the first time during the previous week. For the weekly initial jobless claims, we are mainly concerned about upward shifts because they could have a negative impact on the stability of our society. It is well-known that the initial jobless claims are usually associated with economic conditions. More specifically, the economic policy uncertainty index (X), commonly used in the economic literature as an effective measure of the uncertainty in tax, spending, regulatory, and monetary policies, is believed to contain useful information about the initial jobless claims (cf., Baker et al. 2016). The data of (X, Y) can be downloaded from the web page of the Federal Reserve Economic Data with the link <https://fred.stlouisfed.org>. In this paper, we use the data during 2005-2009, which are shown in Figure 8, to demonstrate the application of the proposed EWMAC chart.

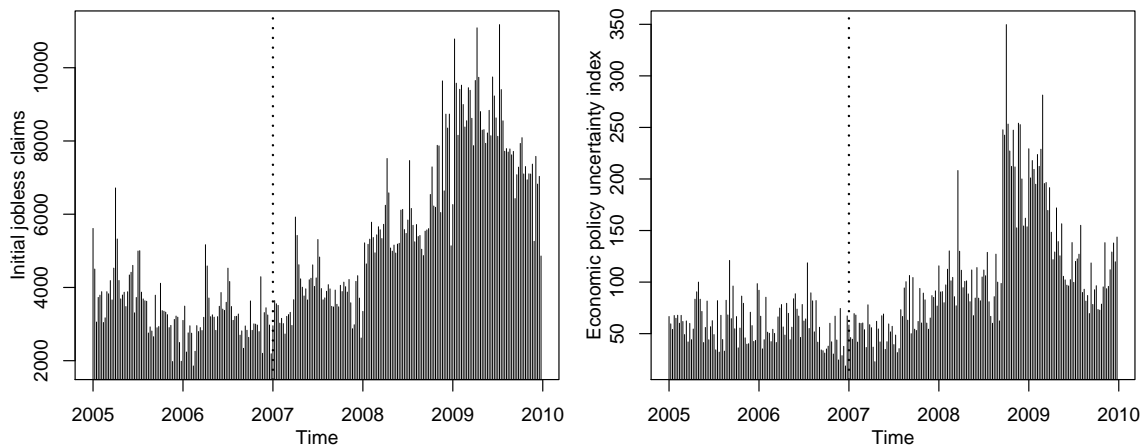


Figure 8: Observed weekly initial jobless claims and economic policy uncertainty index readings in Arizona during 2005–2009. The vertical dotted line in each plot separates the IC data and the data for online monitoring.

In this paper, the proposed EWMAC chart is constructed and designed in cases when process observations are temporally independent. In the current dataset, however, autocorrelation could exist in the observed data and thus it should be properly addressed before the EWMAC chart can be applied. To this end, we consider using the flexible $ARMA(p, q)$ time series model (cf., Box and Jenkins 1976) to describe the data autocorrelation, where p and q are the orders of autoregression

and moving average, respectively. More specifically, the data of X and Y are modelled by two separate ARMA(p, q) models, and the parameters p and q are determined by the popular Bayesian Information Criterion (BIC, Schwarz 1978). The BIC criterion is chosen because of its consistency property in selecting the true model (cf., Yang 2005). After the model selection by BIC, the following ARMA(1,0) model is obtained for describing the observed data of Y :

$$(Y_t - \mu_y)/\sigma_{e,y} = \phi(Y_{t-1} - \mu_y)/\sigma_{e,y} + e_{y,t},$$

where $e_{y,t}$'s are the i.i.d. random errors with mean 0 and variance 1. The estimated values for μ_y , ϕ , and $\sigma_{e,y}$ are $\hat{\mu}_y = 3429.54$, $\hat{\phi} = 0.61$, and $\hat{\sigma}_{e,y} = 649.47$, respectively. Similarly, the following ARMA(0,0) model is obtained for describing the observed data of X :

$$(X_t - \mu_x)/\sigma_{e,x} = e_{x,t},$$

where the estimates of μ_x and $\sigma_{e,x}$ are $\hat{\mu}_x = 60.02$ and $\hat{\sigma}_{e,x} = 20.17$. Then, we can calculate the standardized residuals as follows: for $t \geq 1$,

$$\hat{e}_{y,t} = (Y_t - \hat{\mu}_y)/\hat{\sigma}_{e,y} - \hat{\phi}(Y_{t-1} - \hat{\mu}_y)/\hat{\sigma}_{e,y}, \quad \hat{e}_{x,t} = (X_t - \hat{\mu}_x)/\hat{\sigma}_{e,x}.$$

The time series of the calculated standardized residuals are shown in Figure 9.

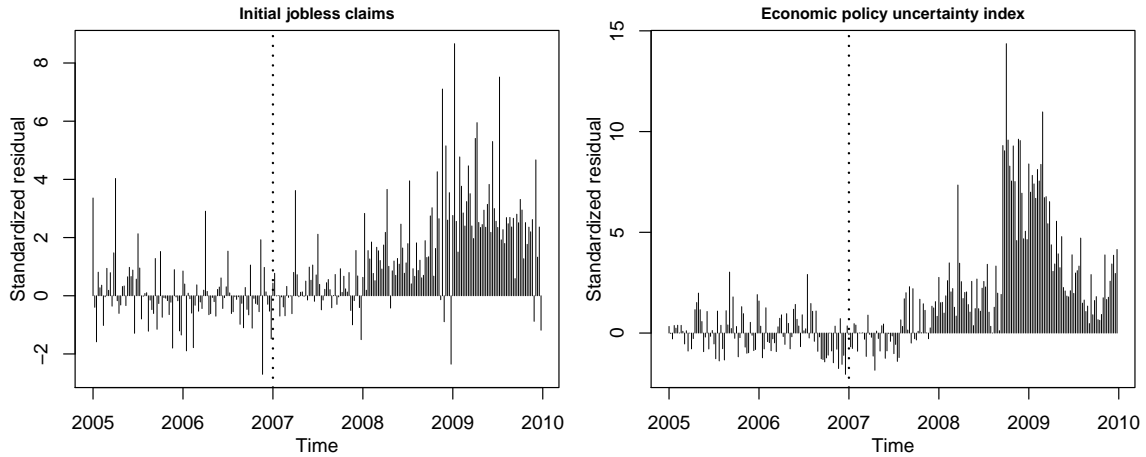


Figure 9: Standardized residuals $\{e_{y,t}\}$ and $\{e_{x,t}\}$ of the weekly initial jobless claim data in Arizona.

It is well demonstrated in the literature that shift detection in the original data is equivalent to shift detection in the residuals obtained from an ARMA model, in the sense that a shift occurs in the original data if and only if there is a shift in the residuals (e.g., Apley and Tsung 2002). Next, we apply the proposed EWMAC chart to the calculated residuals. To this end, the observed

data in years 2005 and 2006 are used as the IC data, which look quite stable in Figures 8 and 9. From the IC data, the IC parameters, including the regression coefficients (β_0, β_1) in the model $\widehat{e}_{y,t} = \beta_0 + \beta_1 \widehat{e}_{x,t} + \varepsilon_t$, can be estimated. The estimated values of (β_0, β_1) are $\widehat{\beta}_0 = -0.02$ and $\widehat{\beta}_1 = 0.085$. Since $\widehat{\beta}_1$ is positive, it can be concluded that the decorrelated observations of Y is positively associated with the decorrelated observations of X , which is consistent with our intuition. In the charts (2)-(3) and (4)-(5), we choose $\lambda = 0.3$, $ARL_{\mathbf{X},0} = ARL_{Y,0} = 200$, and the weighting function to be $\phi_L(x; \lambda, h_{\mathbf{X}})$, as in some simulation examples. Then, the control limits $h_{\mathbf{X}}$ and h_Y can be determined by a bootstrap procedure with the bootstrap sample size of 10,000 from the IC data. Next, the proposed EWMAC chart is used to monitor the residuals $\{e_{y,t}\}$ starting from the 1st week of 2007. The EWMA statistic $E_{\mathbf{X},t}$ for monitoring the decorrelated observations of X and the corresponding weights $\phi_L(E_{\mathbf{X},t}; \lambda, h_{\mathbf{X}})$ are shown in Figure 10. From the left panel of the figure, it can be seen that $E_{\mathbf{X},t}$ is below the control limit $h_{\mathbf{X}}$ during most times in 2007 and exceeds $h_{\mathbf{X}}$ starting from the beginning of 2018. Consequently, from the right panel of the figure, we can see that the weights $\phi_L(E_{\mathbf{X},t}; \lambda, h_{\mathbf{X}})$ used in the chart (4)-(5) are equal to $\lambda = 0.3$ during most times in 2007, and become large starting from the beginning of 2018. The EWMAC charting statistic $E_{Y,t}$ is shown in the top-left panel of Figure 11, and its first signal is given at the 2nd week of 2018. As a comparison, the six competing charts EWMA, AEWMA, MEWMA, RA, ZNO and CSC with $ARL_0 = 200$ and $\lambda = 0.3$ (or $k = 0.3$) are also shown in Figure 11. Their control limits are all determined by the bootstrap procedure with 10,000 bootstrap samples from the IC data. The first signals of the charts EWMA, AEWMA, MEWMA, RA, ZNO and CSC are at the 13th, 13th, 4th, 14th, 7th, and 7th weeks, respectively. So, the first signal by the proposed EWMAC chart is 11 weeks earlier than the ones by EWMA and AEWMA, 2 weeks earlier than the one by MEWMA, 12 weeks earlier than the one by RA, and 5 weeks earlier than the ones by ZNO and CSC. This example illustrates that it is indeed beneficial to use useful information in the weekly readings of the economic policy uncertainty index when detecting an upward shift in the weekly initial jobless claims in Arizona during 2007-2009, because the resulting chart (i.e., EWMAC) can give a signal of the upward shift at least 2 weeks earlier than the competing methods considered, so that Arizona government can make timely interventions to handle the issue of increasing jobless claims.

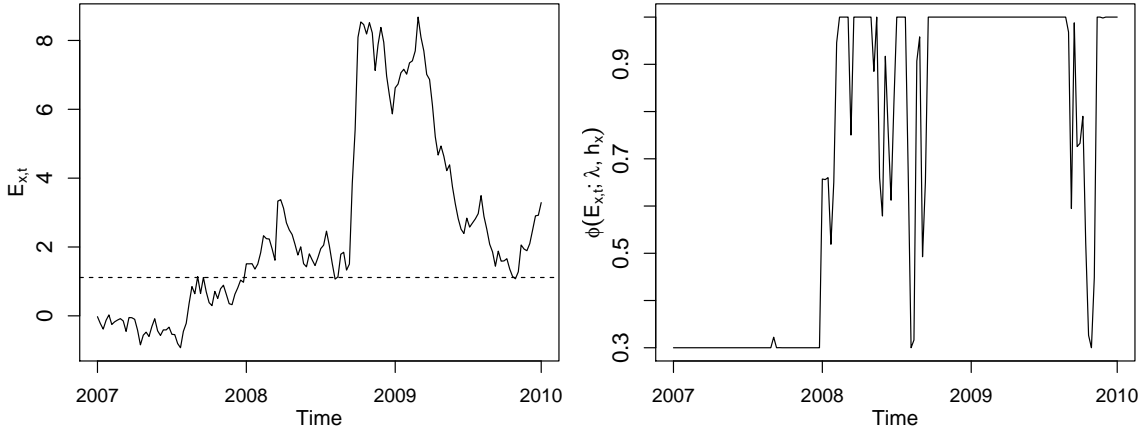


Figure 10: The EWMA statistic $E_{\mathbf{X},t}$ and the corresponding weights $\phi(E_{\mathbf{X},t}; \lambda, h_{\mathbf{X}})$ in the initial jobless claim example. The dashed line in the left panel denotes the control limit $h_{\mathbf{X}}$.

5 Concluding Remarks

We have presented a new SPC methodology for monitoring process performance variables while using helpful information in covariates. This method is appropriate for applications in which only shifts in the performance variables are our major concern and need to be detected promptly, and shifts in the covariates or in the relationship between the performance variables and covariates are either secondary or not our concern at all. Because a shift in the covariates may not necessarily cause a shift in the process performance variables and vice versa in some applications, the process monitoring problem discussed in the paper is quite challenging. The proposed EWMAC charting scheme handles the problem by using the helpful information of covariates in the weighting function (cf., (4)) only. If the covariates tend to have a shift, then the value of this weighting function would be relatively large. Consequently, more weights will be put on the current and several most recent observations of the process performance variables, making the chart more sensitive to a future shift in the process performance variables. However, because the charting statistic in (4) is a weighted average of the observations of the process performance variables, its signals can only be triggered by shifts in the process performance variables. In the previous two sections, it has been shown by some numerical studies that the proposed method is effective in various cases considered.

There are still some issues in the proposed EWMAC chart that need to be addressed in our future research. For instance, three possible weighting functions are considered in the paper (cf., (6)-(8)). It is still unknown to us whether there is any more powerful weighting functions for the

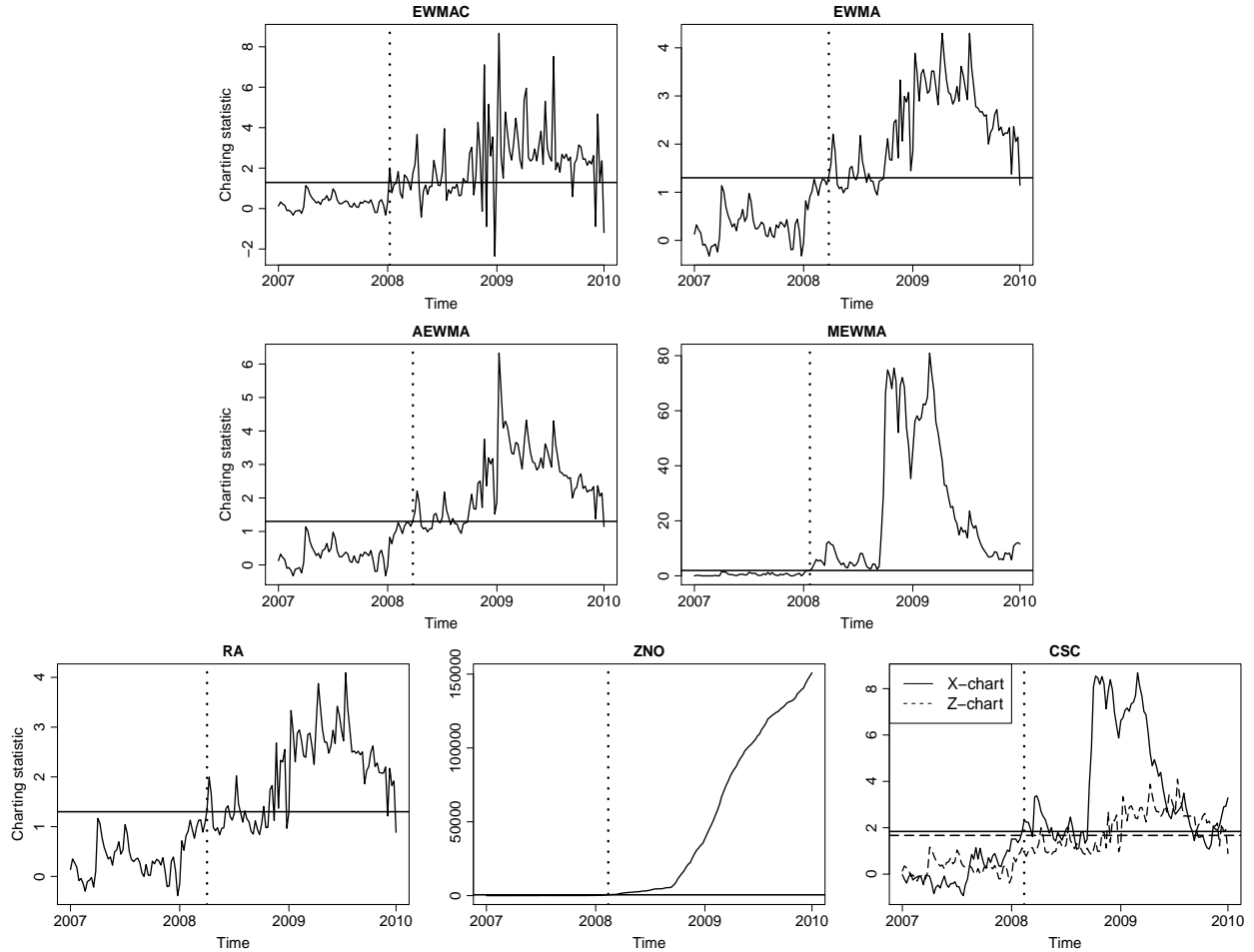


Figure 11: Seven control charts for monitoring the weekly initial jobless claim data in Arizona during 2007-2009. In each plot, the horizontal line(s) denotes the control limit(s), and the vertical dotted line denotes the first signal time of the related control chart.

EWMA chart. In the current method, the weighting function $\phi(E_{\mathbf{X},t}; \lambda, h_{\mathbf{X}})$ is determined based on the covariate information only. Actually, it can also use the helpful information in the past data of Y , as discussed in Li and Qiu (2014). The current EWMA chart is constructed based on the EWMA charting scheme. It is our belief that the idea presented in the paper can also be applied to the CUSUM and CPD charting schemes. But, the details still need to be further developed. Also, similar to a conventional one-sided EWMA chart without using a reflecting barrier, the one-sided EWMA charts discussed in the paper could have the inertia problem (cf., Woodall and Mahmoud 2005). Some modifications might be needed to address this issue (e.g., Yashchin 1993). In addition, although the adaptive weighting approach adopted by the proposed EWMA chart is an effective way to take advantage of the useful covariate information, other strategies like control charts with

variable sampling rates could also be considered in the future research. Finally, as pointed out in Section 2, cases when the process performance variable Y is multivariate, when process observations are correlated over observation times, or when the process IC distribution is time-varying need to be studied carefully in the future research.

Supplementary Materials

supplement.pdf: This document contains some extra numerical results about the control charts discussed in Section 3 of the main paper.

ComputerCodesAndData.zip: This zip file contains the real-data used in Section 4 of the paper, the R code to implement the proposed EWMAC chart, and a brief ReadMe file to explain how to use the R code.

Acknowledgments: The authors thank the editor, the associate editor, and four referees for their constructive comments and suggestions, which improved the quality of the paper greatly. This research is supported in part by the NSF grant DMS-1914639.

References

- Apley D.W., and Tsung, F. (2002), “The autoregressive T^2 chart for monitoring univariate auto-correlated processes,” *Journal of Quality Technology*, **34**, 80–96.
- Asadzadeh S., Aghaie A., and Yang S. (2008), “Monitoring and diagnosing multistage processes: a review of cause selecting control charts,” *Journal of Industrial and Systems Engineering*, **2**, 214–235.
- Baker, S.R., Bloom, N., Davis, S.J. (2016), “Measuring economic policy uncertainty,” *The Quarterly Journal of Economics*, **131**, 1593–1636.
- Beaton, A.E., and Tukey, J.W. (1974), “The fitting of power series, meaning polynomials, illustrated on band-spectroscopic data,” *Technometrics*, **16**, 147–185.
- Bien, J., Taylor, J., and Tibshirani, R. (2013), “A lasso for hierarchical interactions,” *The Annals of Statistics*, **41**, 1111–1141.

- Box, G.E.P., and Jenkins, G.M. (1976), *Time Series Analysis, Forecasting and Control*, San Francisco: Holden-Day.
- Capizzi, G., and Masarotto, G. (2003), “An adaptive exponentially weighted average control chart,” *Technometrics*, **45**, 199–207.
- Capizzi, G., and Masarotto, G. (2008), “Practical design of generalized likelihood ratio control charts for autocorrelated data,” *Technometrics*, **50**, 357–370.
- Chakraborti, S., van der Laan, P. and Bakir, S.T. (2001), “Nonparametric control charts: an overview and some results,” *Journal of Quality Technology*, **33**, 304–315.
- Chatterjee, S., and Qiu, P. (2009), “Distribution-free cumulative sum control charts using bootstrap-based control limits,” *The Annals of Applied Statistics*, **3**, 349–369.
- Cook, R.D., and Weisberg, S. (1999), *Applied Regression Including Computing and Graphics*, New York: John Wiley & Sons.
- Fan, J., and Gijbels, I. (1996), *Local Polynomial Modelling and Its Applications*, Chapman & Hall: London.
- Fan, J., and Li, R. (2001), “Variable Selection via Nonconcave Penalized Likelihood and its Oracle Properties,” *Journal of the American Statistical Association*, **96**, 1348–1360.
- Hastie, T., and Tibshirani, R. (1990), *Generalized Additive Models*, Chapman Hall/CRC: Boca Raton, FL.
- Hawkins, D.M. (1991), “Multivariate quality control based on regression-adjusted variables,” *Technometrics*, **33**, 61–75.
- Hawkins, D.M., and Olwell, D.H. (1998), *Cumulative Sum Charts and Charting for Quality Improvement*, New York: Springer-Verlag.
- Hawkins, D.M., Qiu, P., and Kang, C.W. (2003), “The changepoint model for statistical process control,” *Journal of Quality Technology*, **35**, 355–366.
- Huber, P.J. (1981), *Robust Statistics*, New York: Wiley.

- Jiang, Q., Yan, X., and Huang, B. (2016), "Performance-driven distributed PCA process monitoring based on fault-relevant variable selection and Bayesian inference," *IEEE Transactions on Industrial Electronics*, **63**, 377–386.
- Jiang, W., Wang, K., and Tsung, F. (2012), "A variable-selection-based multivariate EWMA chart for process monitoring and diagnosis," *Journal of Quality Technology*, **44**, 209–230.
- Kang, L., and Albin, S.L. (2000), "On-line monitoring when the process yields a linear profile," *Journal of Quality Technology*, **32**, 418–426.
- Koch, P.D., and Rasche, R.H. (1988), "An examination of the commerce department leading-indicator approach," *Journal of Business & Economic Statistics*, **6**, 167–187.
- Lee, H. C., and Apley, D. W. (2011), "Improved design of robust exponentially weighted moving average control charts for autocorrelated processes," *Quality and Reliability Engineering International*, **27**, 337–352.
- Li, Q., and Racine, J. (2004), "Cross-validated local linear nonparametric regression," *Statistica Sinica*, **14**, 485–512.
- Li, Z., and Qiu, P. (2014), "Statistical process control using dynamic sampling," *Technometrics*, **56**, 325–335.
- Lowry, C.A., Woodall, W.H., Champ, C.W., and Rigdon, S.E. (1992), "A multivariate exponentially weighted moving average control chart," *Technometrics*, **34**, 46–53.
- Montgomery, D.C. (2012), *Introduction to Statistical Quality Control*, New York: John Wiley & Sons.
- Noorossana, R., Saghaei, A., and Amiri, A. (ed.) (2011), *Statistical Analysis of Profile Monitoring*, New York: John Wiley & Sons.
- Page, E.S. (1954), "Continuous inspection schemes," *Biometrika*, **4**, 100–114.
- Paynabar, K., Jin, J., and Yeh, A.B. (2012), "Phase I risk-adjusted control charts for monitoring surgical performance by considering categorical covariates," *Journal of Quality Technology*, **44**, 39–53.

- Paynabar, K., Qiu, P., and Zou, C. (2016), “A change point approach for phase-I analysis in multivariate profiles monitoring and diagnosis,” *Technometrics*, **58**, 191–204.
- Peres, F.A.P., and Fogliatto, F.S. (2018), “Variable selection methods in multivariate statistical process control: A systematic literature review,” *Computers & Industrial Engineering*, **115**, 603–619.
- Qiu, P. (2005), *Image Processing and Jump Regression Analysis*, New York: John Wiley & Sons.
- Qiu, P. (2014), *Introduction to statistical process control*, Boca Raton, FL: Chapman Hall/CRC.
- Qiu, P. (2018), “Some perspectives on nonparametric statistical process control,” *Journal of Quality Technology*, **50**, 49–65.
- Qiu, P., and Hawkins, D. (2001), “A rank based multivariate CUSUM procedure,” *Technometrics*, **43**, 120–132.
- Qiu, P., Li, W., and Li, J. (2020), “A new process control chart for monitoring short-range serially correlated data,” *Technometrics*, **62**, 71–83.
- Qiu, P., and Xiang, D. (2014), “Univariate dynamic screening system: an approach for identifying individuals with irregular longitudinal behavior,” *Technometrics*, **56**, 248–260.
- Qiu, P., Zi, X., and Zou, C. (2018), “Nonparametric dynamic curve monitoring,” *Technometrics*, **60**, 386–397.
- Qiu, P., Zou, C., and Wang, Z. (2010), “Nonparametric profile monitoring by mixed effects modeling (with discussions),” *Technometrics*, **52**, 265–277.
- Roberts S.W. (1959), “Control chart tests based on geometric moving averages,” *Technometrics*, **1**, 239–250.
- Sachlas, A., Bersimis, S. and Psarakis, S. (2019), “Risk-adjusted control charts: theory, methods, and applications in health,” *Statistics in Biosciences*, **11**, 630–658.
- Saleh, N. A., Mahmoud, M. A., Jones-Farmer, L. A., Zwetsloot, I., and Woodall, W. H. (2015), “Another look at the EWMA control chart with estimated parameters,” *Journal of Quality Technology*, **47**, 363–382.

- Shewhart, W.A. (1931), *The Economic Control of the Quality of Manufactured Production*, New York: Macmillan.
- Schwarz, G. (1978), “Estimating the dimension of a model,” *The Annals of Statistics*, **6**, 461–464.
- Steiner, S.H., Cook, R.J., Farewell, V.T., and Treasure, T. (2000), “Monitoring surgical performance using risk-adjusted cumulative sum charts,” *Biostatistics* **1**, 441–452.
- Steiner, S.H., and Jones, M. (2010), “Risk-adjusted survival time monitoring with an updating exponentially weighted moving average (EWMA) control chart,” *Statistics in Medicine*, **29**, 444–454.
- Tibshirani, R. (1996), “Regression Shrinkage and Selection via the LASSO,” *Journal of the Royal Statistical Society, Series B*, **58**, 267–288.
- Wade M.R., and Woodall W.H. (1993), “A review and analysis of cause-selecting control charts,” *Journal of Quality Technology*, **25**, 161–169.
- Wahba, G. (1990), *Spline Models for Observational Data*, CBMS 59, SIAM, Philadelphia.
- Wang, K., and Jiang, W. (2009), “High-dimensional process monitoring and fault isolation via variable selection,” *Journal of Quality Technology*, **41**, 247–258.
- Woodall, W.H., and Mahmoud, M.A. (2005), “The inertial properties of quality control charts,” *Technometrics*, **47**, 425–436.
- Woodall, W. H., Fogel, S. L., and Steiner, S. H. (2015), “The monitoring and improvement of surgical outcome quality,” *Journal of Quality Technology*, **47**, 383–399.
- Yang, Y. (2005), “Can the strengths of AIC and BIC be shared? A conflict between model identification and regression estimation,” *Biometrika*, **92**, 937–950.
- Yashchin, E. (1993), “Statistical control schemes: methods, applications and generalizations,” *International Statistical Review*, **61**, 41–66.
- Zhang G.X. (1984), “A new type of control charts and theory of diagnosis with control charts,” *World Quality Congress Transactions*, American Society for Quality Control, 175–185.
- Zou, H. (2006), “The Adaptive Lasso and its Oracle Properties,” *Journal of the American Statistical Association*, **101**, 1418–1429.

Zou, C., and Qiu, P. (2009), “Multivariate statistical process control using LASSO,” *Journal of the American Statistical Association*, **104**, 1586–1596.

Zou, C., Jiang, W., and Tsung, F. (2011), “A LASSO-based diagnostic framework for multivariate statistical process control,” *Technometrics*, **53**, 297–309.